Remote Sensing of Environment 139 (2013) 97–115

Contents lists available at ScienceDirect

Remote Sensing of Environment

journal homepage: www.elsevier.com/locate/rse

Spatial patterns and temporal dynamics in savanna vegetation phenology across the North Australian Tropical Transect

Xuanlong Ma [a,b,c], Alfredo Huete [b,*], Qiang Yu [b], Natalia Restrepo Coupe [b], Kevin Davies [b], Mark Broich [b], Piyachat Ratana [b], Jason Beringer [d], Lindsay B. Hutley [e], James Cleverly [b,f], Nicolas Boulain [b], Derek Eamus [b,f,g]

[a] Key Laboratory of Water Cycle and Related Land Surface Processes, Institute of Geographic Sciences and Natural Resources Research, Chinese Academy of Sciences, Beijing 100101, China
[b] Plant Functional Biology and Climate Change Cluster (C3), University of Technology, Sydney, NSW 2007, Australia
[c] University of Chinese Academy of Sciences, Beijing 100049, China
[d] School of Geography and Environmental Science, Monash University, Melbourne, Victoria 3800, Australia
[e] Research Institute for the Environment and Livelihoods, Charles Darwin University, Casuarina, Northern Territory 0909, Australia
[f] Australian Supersite Network, Terrestrial Ecosystem Research Network, University of Technology, Sydney, NSW 2007, Australia
[g] National Centre for Groundwater Research and Training, University of Technology, Sydney, NSW 2007, Australia

ARTICLE INFO

Article history:
Received 4 December 2012
Received in revised form 22 July 2013
Accepted 23 July 2013
Available online xxxx

Keywords:
Savannas
Phenology
MODIS
EVI
Eddy covariance
Climate change
NATT

ABSTRACT

The phenology of a landscape is a key parameter in climate and biogeochemical cycle models and its correct representation is central to the accurate simulation of carbon, water and energy exchange between the land surface and the atmosphere. Whereas biogeographic phenological patterns and shifts have received much attention in temperate ecosystems, much less is known about the phenology of savannas, despite their sensitivity to climate change and their coverage of approximately one eighth of the global land surface. Savannas are complex assemblages of multiple tree, shrub, and grass vegetation strata, each with variable phenological responses to seasonal climate and environmental variables. The objectives of this study were to investigate biogeographical and inter-annual patterns in savanna phenology along a 1100 km ecological rainfall gradient, known as North Australian Tropical Transect (NATT), encompassing humid coastal *Eucalyptus* forests and woodlands to xeric inland *Acacia* woodlands and shrublands. Key phenology transition dates (start, peak, end, and length of seasonal greening periods) were extracted from 13 years (2000–2012) of Moderate Resolution Imaging Spectroradiometer (MODIS) Enhanced Vegetation Index (EVI) data using Singular Spectrum Analysis (SSA).

Two distinct biogeographical patterns in phenology were observed, controlled by different climate systems. The northern (mesic) portion of the transect, from 12°S, to around 17.7°S, was influenced by the Inter-Tropical Convergence Zone (ITCZ) seasonal monsoon climate system, resulting in strong latitudinal shifts in phenology patterns, primarily associated with the functional response of the C4 grass layer. Both the start and end of the greening (enhanced vegetation activity) season occurred earlier in the northern tropical savannas and were progressively delayed towards the southern limit of the *Eucalyptus*-dominated savannas resulting in relatively stable length of greening periods. In contrast, the southern xeric portion of the study area was largely decoupled from monsoonal influences and exhibited highly variable phenology that was largely rainfall pulse driven. The seasonal greening periods were generally shorter but fluctuated widely from no detectable greening during extended drought periods to length of greening seasons that exceeded those in the more mesic northern savannas in some wet years. This was in part due to more extreme rainfall variability, as well as a C3/C4 grass-forb understory that provided the potential for extended greening periods. Phenology of *Acacia* dominated savannas displayed a much greater overall responsiveness to hydroclimatic variability. The variance in annual precipitation alone could explain 80% of the variances in the length of greening season across the major vegetation groups. We also found that increased variation in the timing of phenology was coupled with a decreasing tree-grass ratio. We further compared the satellite-based phenology results with tower-derived measures of Gross Ecosystem Production (GEP) fluxes at three sites over two contrasting savanna classes. We found good convergence between MODIS EVI and tower GEP, thereby confirming the potential to link these two independent data sources to better understand savanna ecosystem functioning.

1. Introduction

Phenology is the study and analysis of the life cycles of flora and fauna and their interactions with climate and other seasonal

---

[*] Corresponding author at: Plant Functional Biology and Climate Change Cluster (C3), University of Technology, Sydney, Broadway, NSW 2007, Australia. Tel.: +61 2 9514 4084.
E-mail address: alfredo.huete@uts.edu.au (A. Huete).

0034-4257/$ – see front matter © 2013 Elsevier Inc. All rights reserved.
http://dx.doi.org/10.1016/j.rse.2013.07.030

environmental drivers (White & Thornton, 1997). Studies involving species-level phenology as well as at community-level, ecosystem and biome scales, are important in global land-surface change research. As an integrative indicator of climate variability and vegetation growth responses to climate change, understanding the timing and drivers of phenological patterns is also required to better simulate the carbon, water, and energy exchanges between atmosphere and land surface (Running & Hunt, 1993).

Phenological studies of vegetation can be carried out at the species level (bud break, flowering, leaf flush, etc.) using in-situ field techniques (Menzel et al., 2006; Williams, Myers, Muller, Duff, & Eamus, 1997). However, remote sensing provides the only feasible means of phenology monitoring over landscape, continental and global scales (Ahl et al., 2006; Glenn, Huete, Nagler, & Nelson, 2008; Huete et al., 2002; Stockli & Vidale, 2004; Zhang et al., 2003). Space-borne optical sensors such as NOAA-AVHRR and NASA-MODIS provide daily measurements of a variety of biophysical and biochemical satellite-based parameters of the land surface (Friedl et al., 2002; Huete et al., 2002; Tucker, Townshend, & Goff, 1985). These earth observation systems examine broader scale phenomena that allow retrievals of whole-system phenological metrics, such as the timing and magnitudes of greening, peak activity, and drying phases of the growing season (Zhang et al., 2003).

Many remote sensing phenology studies have been conducted in northern mid- to high-latitude temperate regions in which the timing and duration of the growing season is tightly correlated with temperature (Chen, Hu, & Yu, 2005; de Beurs & Henebry, 2005; Piao, Fang, Zhou, Ciais, & Zhu, 2006; White et al., 2009; Zhang, Friedl, Schaaf, & Strahler, 2004). In contrast to temperature-driven patterns in vegetation phenology, there have been fewer studies conducted in tropical water- or light- limited/driven ecosystems. The start of the rainy season has been found to be the best predictor of the onset of vegetation green-up in drier areas where water availability is the primary driver of vegetation growth (Brown, de Beurs, & Vrieling, 2010; Zhang, Friedl, Schaaf, Strahler, & Liu, 2005). In light-limited areas of the Amazon Basin, the green-up phenophase in rainforests was found to be synchronized with the dry season, when sunlight availability increases (Huete et al., 2006).

“Savanna” as an ecological term has various definitions (Gillison, 1981; Walker & Gillison, 1982; Frost et al., 1986; Scholes & Walker, 1993; Eamus & Prior, 2001). In this study, we adopted a definition after Walker and Gillison (1982), who defined savannas as wooded communities with a conspicuous perennial or annual graminoid component. In an Australian context, such a definition has been further extended to include woodland savanna (single-stemmed woody) and shrub savanna (multi-stemmed woody) ecosystems (Walker & Gillison, 1982). We adopted such a definition due to its recognition of varying mixtures of trees, shrubs and graminoids that form a structural continuum (Walker & Gillison, 1982).

The tree-shrub-grass layers of savanna have distinct physiological characteristics, expressed as multiple plant functional types with tree and grass ratios of cover and leaf area index varying significantly among different savanna classes (Scholes & Archer, 1997). The phenology of mixed physiognomy savanna ecosystems is distinct from those of forests and grasslands. The multi-stratum nature of savannas results in a more complex and dynamic landscape with each layer exhibits unique functional responses and interactions to seasonal rainfall and other environmental variables (Scholes & Archer, 1997).

Savanna phenology has been investigated at species and community scales (Seghieri et al., 2009; Williams et al., 1997). For example, at a site near Darwin (Northern Territory, Australia), ground observations showed evergreen species continued to flush and produce leaves throughout the dry season, and that leafing in brevi- and semi-deciduous species commenced prior to the arrival of rainfall (Williams et al., 1997). In contrast, the fully deciduous species displayed a range of behaviors: some flushed before the first rain, while others flushed after ~25 mm of rain had fallen (Williams et al., 1997). A study conducted at Kruger National Park in South Africa identified two distinct phenological syndromes where leaf flushing of trees occurred prior to rainfall but grasses flush followed the rain (Higgins, Cartay, February, & Combrink, 2011).

At regional scales, savanna phenology has also been investigated using remote sensing (Archibald & Scholes, 2007; Chidumayo, 2001; Ferreira & Huete, 2013; Higgins et al., 2011; Ratana, Huete, & Ferreira 2005). In South African savannas, a model based on AVHRR and MODIS observations can predict 86% of the onset of tree species green-up from day length alone, while with the incorporation of soil moisture the model could predict 73% of the grass green-up, both to within an accuracy of less than one month (Archibald & Scholes, 2007). However, Seghieri et al. (2009) found the phenophases of most Sahelian woody species to be correlated with temperature rather than rainfall. In central Brazil, temporal profiles of vegetation indices over the cerrado exhibited high wet-dry season contrasts, and variations in seasonal vegetation indices (VI) were negatively correlated with woody cover (Ratana et al., 2005). Hill et al. (2011) investigated the utility of MODIS VIs to classify global savanna ecoregions based on annual average phenological profiles. Based on in-situ survey and satellite observations, Hüttich et al. (2009) classified savanna vegetation in South Africa using phenological metrics. Donohue, McVicar, and Roderick (2009) recognized the distinct seasonal contributions of the tree and grass layers in Australian savannas and decomposed AVHRR-NDVI (Normalized Difference Vegetation Index) into recurrent and persistent components, as surrogates of the herbaceous understorey and evergreen woody overstorey, respectively.

However, accurate and robust regional-scale retrievals of savanna phenology metrics remain a challenge using remote sensing methods. For example, in African savannas, Hmimina et al. (2013) found that NDVI time series could not be modeled with sigmoidal functions, as commonly applied to VI time series in temperate biomes (Soudani et al., 2008; Zhang et al., 2003). This was attributed to irregular rainfall driven temporal vegetation growth patterns in savannas, thus requiring use of non-parametric methods, such cubic spline methods, to smooth the VI time series for retrieval of phenology metrics (Hmimina et al., 2013). Jin et al. (2013) coupled flux tower measurements of productivity with MODIS data and similarly found existing phenology retrieval methods were highly unstable across different savanna woodlands sites. These studies suggest a need to consider the limitations of current methodologies and develop more robust and accurate remote sensing methods to retrieve phenological information in savannas landscapes.

Savannas are most commonly found in the tropics and sub-tropics and are present in both mesic and xeric regions (Eamus & Prior, 2001; Frost et al., 1986). Savannas typically experience highly seasonal rainfall and prominent inter-annual climate variability, making them one of the most dynamic global biomes (Frost et al., 1986). With their distinct rainy season and pronounced dry season, they are also considered particularly vulnerable to climate change (Field, Lobell, Peters, & Chiariello, 2007). The biotic and abiotic controls on savanna productivity exhibit high spatial variability and complex interactions that create considerable challenges to accurate simulation of savanna-atmosphere exchange processes (Kanniah, Beringer, & Hutley, 2010; Whitley et al., 2011).

Savannas cover one eighth of the global land area (Scholes & Archer, 1997) and contribute approximately 30% of all terrestrial ecosystem gross primary productivity (House & Hall, 2001). Most importantly, savannas support a vast and ever increasing human population that is supported by livestock grazing activities (Scholes & Archer, 1997). Land degradation in savanna regions has resulted in altered species composition and declines in productivity, which pose concerns for their fate, functioning, and resilience under future climate change (Scheiter et al., 2012), as well as their continued capacity to support human livelihoods and biodiversity (Frost et al., 1986; Hanan & Lehmann, 2011; Scholes & Archer, 1997).

Despite the global importance and vulnerability to anthropogenic influences of savannas, the detailed characterization of biogeographical patterns in their phenological cycles is lacking, particularly at landscape and regional scales. This greatly hampers an effective understanding of future climate impacts on composition, functioning, and fire behavior of savanna systems. There is mounting evidence that savanna systems will be substantially modified by climate change (Scholes & Archer, 1997; Scholes & Parsons, 1997; Bowman et al. 2010; Bowman, Murphy, & Banfai, 2010; Hill & Hanan, 2013), yet there is a lack of knowledge and insufficient data to predict the nature of these changes. Advances made here would have applications for mixed tree/shrub/grass ecosystems globally.

In contrast to savannas in South America and Africa, Australian savannas are largely ecologically intact with relatively low levels of fragmentation (Beringer, Hutley, Hacker, Neininger, & Paw, 2011; Woinarski, Mackey, Nix, & Traill, 2007), enabling a greater capacity to understand the environmental determinants on their growth and functioning. They provide an ideal "living laboratory" to investigate the critical environmental determinants of their phenology and biogeographical variations (Hutley, Beringer, Isaac, Hacker, & Cernusak, 2011; Williams, Duff, Bowman, & Cook, 1996). In this study, we utilized satellite observations to investigate the biogeographic patterns and inter-annual variations of vegetation phenology across an 1100 km north Australian ecological rainfall transect (known as NATT). This transect encompassed a transitional gradient from coastal mesic *Eucalyptus* dominated forests and woodlands to inland xeric *Acacia* dominated woodlands, shrublands and grasslands (Walker, Steffen, Canadell, & Ingram, 1999).

Numerous studies have been made across this transect involving biogeography, soils, ecophysiology, meteorology and land-atmosphere exchange processes (see review by Hutley et al., 2011). The use of terrestrial transects has been widely adopted by the global change community as a method to assess spatial patterns of biogeochemical processes (Koch, Vitousek, Steffen, & Walker 1995; Walker et al., 1999). The spatial variation of long-term trends in precipitation and phenology along transects can be used as surrogates for predicting future climatological variations to understand the possible responses of ecosystems to global change (Koch et al., 1995). Future climate is expected to exhibit more inter-annual variability with increasing number of extreme meteorological events (Easterling et al., 2000; Seager, Naik, & Vogel, 2013), which are likely to impact on savanna phenology.

The objectives of this study were to (1) determine the variations in timing and duration of key vegetation phenological phases along a rainfall gradient (NATT); (2) assess the interactions and relative roles of vegetation structural classes and rainfall on savanna phenology; and (3) investigate the inter-annual rainfall responses and variations of vegetation phenology to decadal rainfall variability.

2. Data and methods

2.1. Study area

This study focused on a sub-continental scale ecological rainfall gradient of more than 1100 km in length, known as the North Australian Tropical Transect (NATT) (Koch et al., 1995), that encompassed an area of 1.38 million km^2 between 12°S to 23°S and 128°E to 138°E (Fig. 1). The NATT was conceptualized in the mid-1990s as part of the International Geosphere Biosphere Programme (IGBP) (Koch et al., 1995), together with the Kalahari transect in southern Africa and the SALT (Savanne à Long Terme) transect in West Africa, these three major transects have been used extensively in the study of global savannas (Beringer, Hutley, Hacker, Neininger, & Paw, 2011; Bowman, Wilson, & Dunlop, 1988; Cook, Williams, Hutley, O'Grady, & Liedloff 2002; Eamus, Boulain, Cleverly, & Breshears, 2013; Eamus, Cleverly, et al., 2013; Hutley et al., 2011; Scholes & Parsons, 1997; Walker et al., 1999; Williams et al., 1996).

The NATT region is characterized as having a classic monsoon climate pattern with reversal of flow from low-level continental-origin easterlies during winter to low-level westerly flow during summer (December-March) (Suppiah, 1992). Mean annual precipitation (2000–2012) decreases from over 1700 mm in the northern mesic tropics to about 300 mm in the xeric southern region. Inter-annual variations in rainfall (2000–2012) range from less than 30% of the mean (coefficient of variation, CV) to more than 60% CV from north to south. Soils are ranging from Kandosol (Palexeralf in U.S. Taxonomy) and affiliated types at the northern humid end of the transect (Hutley et al., 2011), to black cracking clay soils or sandy soils at the southern arid end (Walker et al., 1999). Extensive grazing and limited horticulture are the primary land-use types (Hutley et al., 2011) and frequent fires occur annually in the dry season of the higher-rainfall areas, associated with higher fuel loads (Anderson et al., 1998).

Within this extensive transect study area, we selected six well-characterized local sites, as described in Beringer, Hutley, Hacker, Neininger, and Paw (2011), representing different vegetation structures/functional types and precipitation regimes, to investigate variations in phenology across savanna vegetation classes (Table 1). These sites include several eddy covariance flux towers that can be used for the assessment of satellite observed vegetation seasonality and retrievals of phenology events, from north to south: Howard Springs, Adelaide River, Daly River, Dry River, Sturt Plains and Ti Tree. We note that the Sturt Plains site, which is classified as tussock grassland, is not a savanna since crown cover of the woody components is usually below 0.2% in this vegetation type (Walker & Gillison, 1982), but we included it in our analysis as an extreme end-member of the tree-shrub-grass continuum.

The vegetation of the entire transect study area follows a wet-dry savanna gradient that transitions from *Eucalyptus* dominated forests and woodlands in the northern areas to *Acacia*-dominated woodlands and shrublands to the south. The northern tropical savannas are dominated by an overstorey of evergreen *Eucalyptus* and *Corymbia* species, with a middle layer of pan tropical semi- to fully deciduous tree and shrub species, and understorey of annual and perennial C4 grasses (Egan & Williams, 1996; Hutley et al., 2011). The dominance of *Eucalyptus* species declines sharply at around 18°S, and transitions into drier *Acacia* dominated woodlands/shrublands, and hummock grasslands (Bowman, 1996), with perennial grass species becoming more abundant in the understorey (Walker et al., 1999). This pattern of annual grasses at the wet end (Howard Springs) and perennial at the dry end (Alice Springs) is unique in the world's savannas (Walker et al., 1999).

The herbaceous layer consists of tall grass (height > 100 cm) genera in northern monsoonal areas, including *Sorghum* (annual), *Themeda* and *Heteropogon*, which exhibit marked growth seasonality (McKeon et al., 1990; Walker & Gillison, 1982). These grade into mid-size grasses (30–100 cm) further south, in which *Aristida pruinosa* dominates the understorey in Eucalypt woodlands (NVIS, 2007; Walker & Gillison, 1982). The tussock grasslands are dominated by annual *Iseilema sp.*, perennial *Astrebla sp.* and legume forbs that exhibit less marked growth seasonality (McKeon et al., 1990; Walker & Gillison, 1982). In the extensive south and western areas, hummock grasslands (spinifex) are found consisting of mid-size perennial grasses (hard-leaved *Triodia* spp. and soft-leaved *Plectrachne* spp.) with less marked seasonality (Walker & Gillison, 1982). In the most southern portion of the transect, *Acacia* open woodlands and *Acacia* shrublands (Fig. 1) form a non-overlapping mosaic with hummock grasslands (Nicholas, Franklin, & Bowman, 2011), the understorey grasses are dominated by mid-short C3 and C4 grasses such as *Eragrostis sp.*, *Aristida ramosa*, *Thyridolepis mitchelliana*, and *Stipa sp.* (perennial) with low seasonality in growth (NVIS, 2007; Walker & Gillison, 1982).

Nine major vegetation groups are present in this study area (Table 1), based on growth form, structure and floristic composition (Australian National Vegetation Information System, NVIS, version 4.1). The dominant classes were tropical Eucalypt woodlands, Eucalypt

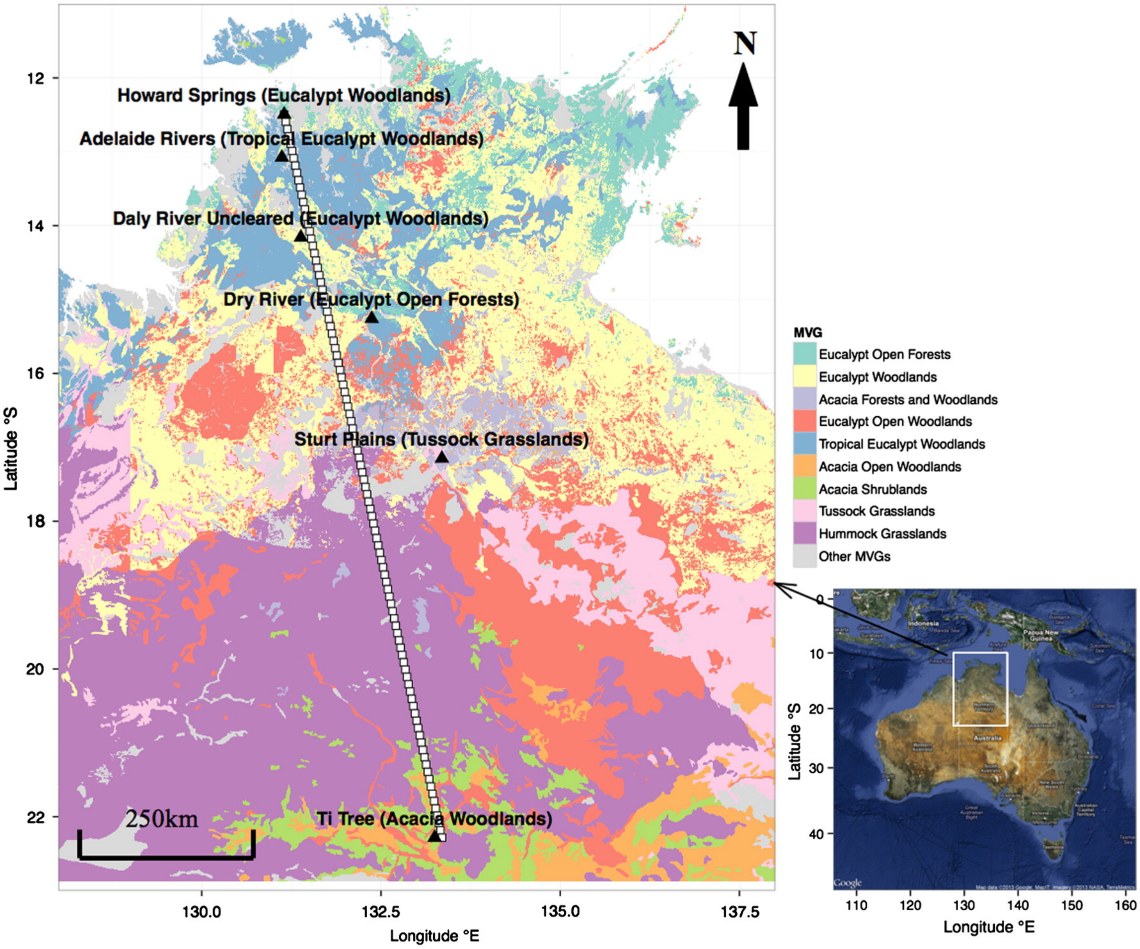

Fig. 1. Spatial extent of the North Australian Tropical Transect (NATT) study area. Six local sites have been labeled on the figure. White solid squares show the 100 pixel samples (sized-up for visualization) from Howard Springs (131.150°E, 12.495°S) to Ti-Tree (133.249°E, 22.283°S) along the NATT. Background is the Australian Major Vegetation Map (MVGs), provided by Australian National Vegetation Information System. Right small panel shows the locations of the study area over Australian continent (image source: Google Earth).

woodlands, Eucalypt open woodlands, Eucalypt open forests, hummock grassland, *Acacia* forests and woodlands, *Acacia* open woodlands, and *Acacia* shrublands (Table 2). The major difference between tropical Eucalypt woodland and Eucalypt woodland is the presence of tall annual bunch-grass (notably *Sorghum* spp.) in the former, and more grass and shrubs in the latter. Geographically, tropical Eucalypt woodlands is primarily distributed in the north-west humid monsoonal areas within 1200–1600 mm Mean Annual Precipitation (MAP), and the Eucalypt woodlands is mainly distributed more south and east, within 800–1200 mm MAP (Fig. 1).

2.2. Satellite data

The Enhanced Vegetation Index (EVI) is widely used as proxy of canopy "greenness", which is defined as an integrative composite property of green leaf area, green foliage cover, structure, and leaf chlorophyll content (Glenn et al., 2008; Huete et al., 2002). In this study, thirteen years (18 Feb 2000–22 Mar 2013) of MODIS EVI products were obtained from USGS repository (ftp://e4ftl01.cr.usgs.gov): 16-day 250 m (MOD13Q1; Collection 5, tiles H29V11, H30V10, H30V11 and H31V11 of MOD13Q1) and 0.05° spatial resolution (MOD13C1). We used the 250 m resolution product to investigate site-level phenological patterns and the 0.05° resolution product to assess regional phenological patterns. EVI was used as a vegetation index that optimizes the combination of reflectance in the red and near-infrared (NIR) bands, based on a 1st-order Beer's law application of canopy radiative transfer that effectively reduces soil background influences and atmospheric noise variations present over the >1100 km transect (Huete, 1988; Huete et al., 2002, 2008). The equation defining EVI is:

$$\mathrm{EVI} = 2.5\frac{\rho_{\mathrm{NIR}} - \rho_{\mathrm{red}}}{\rho_{\mathrm{nir}} + 6\rho_{\mathrm{red}} - 7.5\rho_{\mathrm{blue}} + 1} \tag{1}$$

where ρ_{NIR}, ρ_{red}, and ρ_{blue} are reflectances in the near infrared, red and blue bands respectively (Huete et al., 2002). For each site, to match the footprint of eddy flux tower, a 3 × 3 pixel window (0.5625 km2) was used to extract the EVI time series from MOD13Q1. Residual cloud and aerosol contamination in the original EVI time series were filtered out based on the quality assurance (QA) flags provided with the MOD13Q1 and MOD13C1 products. Gaps remaining after QA filtering were then filled by linear interpolation in the temporal dimension but pixels with more than two consecutive gaps were excluded from the analysis.

2.3. Phenology metrics retrieval

To reduce noise and uncertainties in the MODIS time series data, we employed a data adaptive analysis method, the Singular Spectrum Analysis (SSA), known to be well suited to the analysis of nonlinear dynamics in geophysical datasets (Aban & Tateishi, 2004; Buermann, 2002; Elsner & Tsonis, 1996; Ghil et al., 2002; Kondrashov & Ghil, 2006; Wang & Liang, 2008).

The fundamental concept of SSA is to embed a time series $F = (f_0,\ldots f_{N-1}, fn \in \mathbf{R})$ into high-dimensional Euclidean space and identify

Table 1
Summary of major vegetation groups in the NATT study area.

MVG	Coverage (%)	MAP ± σ (mm)[a]	CV_{MAP} ± σ (%)[a]	Overstorey[b]	Understorey[b]
Eucalypt open forest	4.21	1392 ± 237	27 ± 5	*E. tetrodonta*, *E. miniata*, *E. nesophila*	*Triodia* spp., *Plectrachne* spp., *Sorghum* spp.
Tropical eucalypt woodlands	8.07	1311 ± 259	25 ± 5	*E. tectifica*, *E. tetrodonta*, *E.miniata*, *C. dichromophloia*	*Sorghum* spp., *Triodia* spp., *Chrysopogon* spp.
Eucalypt woodlands	20.79	1025 ± 228	32 ± 7	*E. tetrodonta*, *E. miniata*, *C. dichromophloia*, *C. polycarpa*, *C. bella*	*T. triandra*, *Heteopogon* spp., *Sorghum* spp., *S. fragile*
Eucalypt open woodlands	14.48	685 ± 251	42 ± 11	*C. dichromophloia*, *E. tetrodonta*, *E. miniata*, *C. terminalis*, *E. pruinosa*	*Sorghum* spp., *Heteopogon* spp., *Chrysopogon* spp., *Bothriochloa* spp., *Aristida spp.*
Acacia forests and woodlands	2.04	811 ± 98	36 ± 5	*A. shirleyi*, *A. catenulate*, *A. aneura*, *A. cambagei*, *A. harhophylla*	*Eremophila* spp., *Dodonaea* spp., *Atriplex* spp., *Triodia* spp., *Plectrachne*
Tussock grasslands	7.57	596 ± 152	43 ± 9		*Astrebla* spp., *Austrodanthonia* spp., *Austrostiha* spp., *Dicanthium* spp.
Hummock grasslands	28.75	509 ± 111	49 ± 8	*C. decaisneana*, *E. gongylocarpa*, *A. aneura*	*Plectrachne schinzii*, *T. pungens*, *T. basedowii T. irritans*
Acacia open woodlands	2.81	379 ± 59	60 ± 10	*A. aneura*, *A. georginae*, *A. tephrina*, *A. cam bagei*, *A. harpophylla*	*Atriplex* spp., *Maireana* spp., *Sclerolaena* spp., *Triodia* spp., *Eragrostic* spp.
Acacia shrublands	2.89	405 ± 92	55 ± 9	*A. aneura*, *A. cambadgei*, *A. victoriae*, *A. brachystachya*, *A. resinomarginea*	*Triodia* spp., *Atriplex*

[a] MAP = mean annual precipitation, calculated using BoM gridded rainfall data for every pixel of each vegetation group and then aggregated to obtain MAP for each group. We used 12 hydrological years (2000.07.01-2012.06.30) precipitation data to calculate mean annual precipitation (Jones et al., 2007).

[b] Species information of overstorey and understorey of each vegetation group is cited from NVIS (2007).

the sub-space corresponding to the component of interest from which a reconstructed time series is generated (Alexandrov, 2009). The time series data *F* was first decomposed into $L \times K$ matrix and a window length *L* was defined, so the time series can be constructed to a trajectory matrix $X \in \mathbf{R}$, $K = N - L + 1$ (Hankel matrix) (Alexandrov, 2009). Then Singular Value Decomposition (SVD) is applied to X, and *j*-th eigenvalue λj and eigenvector *Uj* of XXT specify the *j*-th component of the SVD (Alexandrov, 2009):

$$\mathrm{X} = \sum_{j=1}^{d} \sqrt{\lambda_j} U_j V_j^{\mathrm{T}}, \quad V_j = \mathrm{X}^{\mathrm{T}} / \sqrt{\lambda_j}, \quad d = \max j : \lambda_j > 0 . \tag{2}$$

The SSA-based reconstruction then combines the selection of a sub-group SVD components, hankelization of the matrix X from the selected sub-group, and reconstruction of a time series from the matrix X into a length *N* time series (Alexandrov, 2009).

The benefit of using SSA to reduce the uncertainties in a time series is that the first few SVD components of the matrix contain most of the information of the trend and periodicity of the time series while the remaining components contain most of the noise (Ghil et al., 2002). In contrast to linear filtering or wavelet methods, SSA is not a local method because it considers the whole time series while conducting the reconstruction and is therefore, more robust to outliers (Alexandrov, 2009) that may be present in the satellite data due to cloud or aerosol contaminations.

SSA implementation requires two important parameters to be determined: the window length *L* and the selection of the leading components. In testing our dataset, an optimized window length of 37 composite periods (37 × 16 / 365 ≈ 1.6 years) was found to best capture the periodicity and reduce most of the random noise. We selected four leading components to reconstruct the EVI time series, with the first component contributing with information on the long term trend and the remaining components contributing with periodicities of declining frequency, which are important for retrievals of the phenological metrics. Lastly, the SSA reconstructed 16-day MODIS EVI time series was interpolated to daily values using local polynomial regression before being used to derive the phenological metrics.

The biological interpretations of satellite-based phenology for the savanna classes in our study area differ from those used in temperate forests and grasslands. The tree layer is predominantly evergreen and functionally active year round (Hutley, O'Grady, & Eamus, 2001; O'Grady et al., 2009), without a dormant period of below 0 °C temperatures nor periods of significant leaflessness. The start, peak, and end of seasonal vegetation cycles are therefore mostly associated with the functioning of the recurrent grass and forb layers, consisting of C3 and C4 annual and perennial species. The key phenological metrics retrieved with the MODIS time series data were defined as:

- Start of Greening Season (SGS): the beginning date of enhanced seasonal vegetation productivity associated with one or more of the vegetation strata;
- Peak of Greening Season (PGS): the date of maximum vegetation productivity for the savanna vegetation assemblage;

Table 2
Summary of six major NATT sites.

Site	Longitude (°E)	Latitude (°S)	Elevation (m)	MVG	Overstorey	Understorey	Canopy height (m)[a]	Soil[a]	MAP ± σ (mm)[b]
Howard Springs	131.150	12.495	64	Eucalypt woodlands	*E. miniata*, *E. chlorostachys*, *T. ferdinandiana*	*Sorghum* spp.	18.9	Red kandosol	1722 ± 341
Adelaide Rivers	131.118	13.077	90	Tropical eucalypt woodlands	*E. tectifica*, *P. careya*, *B. obovata*	*Sorghum* spp.	12.5	Yellow hydrosol	1692 ± 373
Daly River	131.383	14.159	52	Eucalypt woodlands	*T. grandiflora*, *E. tetrodonta*, *E. latifolia*	*Sorghum* spp., *H. triticeus*	16.4	Red kandosol	1295 ± 334
Dry River	132.371	15.259	175	Eucalypt open forests	*E. tetrodonta*, *E. dichromophloia*, *C. terminnalis*	*Sorghum*. spp., *T. triandra*, *C. fallax*	12.3	Red kandosol	1063 ± 277
Sturt Plains	133.350	17.151	210	Tussock grasslands	–	*Astrebla* spp.	0.1	Gray vertosol	778 ± 304
Ti Tree	133.249	22.283	606	*Acacia* woodlands	*C. opaca*, *E. victrix*, *A. aneura*	*P. latifolia*, *T. mitchelliana*, *E. eriopoda*, *E. pulchella*	6.5	Red kandosol	443 ± 222

[a] Cited from OZFlux website: www.ozflux.org.au.

[b] MAP = mean annual precipitation, calculated using BoM gridded rainfall data for each site using data of 12 hydrological years (2000.07.01-2012.06.30) (Jones et al., 2009).

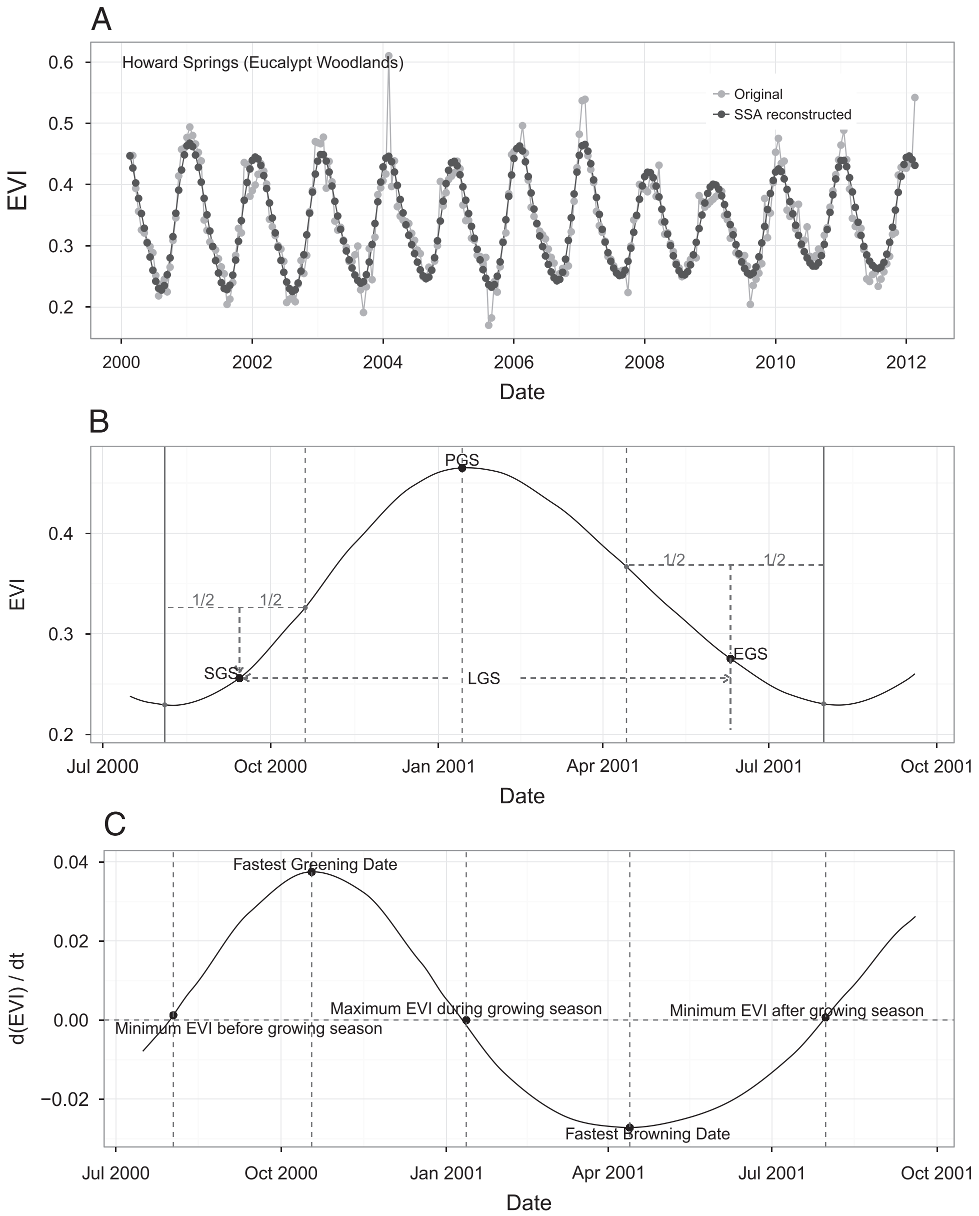

Fig. 2. Phenological methodology schematic diagrams. (A) Original MODIS EVI time series (solid light gray line) with SSA reconstructed time series (solid black line) for Howard Springs from 2000.02.18 to 2012.02.18; (B) SSA reconstructed MODIS EVI time series of one growth cycle (2000–2001) from above time series; (C) One day lag difference (approximation of first derivative) of 2000–2001 SSA reconstructed EVI time series. In panel (B), the phenological metrics have been labeled on the graph. In panel (C), the inflection points, which represent some critical points during a growing cycle, have also been labeled on the graph.

- End of Greening Season (EGS): the end date of enhanced seasonal vegetation productivity associated with one or more of the vegetation strata;
- Length of Greening Season (LGS): the duration of enhanced vegetation productivity, defined as the difference between the end and start of the greening period.

The SSA method for retrievals of phenology transition dates is presented diagrammatically in Fig. 2. An SSA reconstructed sample time series shown alongside the original EVI time series for the Howard Springs site is presented in Fig. 2A. The phenology metrics retrieved (SGS, PGS, EGS, and LGS) are shown for a single year (2000–01) greening cycle from the Howard Springs time series data (Fig. 2B). Their derivations based on inflection points identified by the first derivative of EVI time series are shown in Fig. 2C, which include several critical points: the minimum EVI date prior to the growing season, the date of the fastest growth rate during the green-up period, the date of peak growing season EVI, the date of most rapid brown-down rate (senescence), and the minimum EVI after the cessation of the growing season (Fig. 2C). We assume that the onset of the growing season should occur after the minimum EVI date preceding the growing season, but before the fastest growing date during the green-up period. The start of the greening season (SGS) date is defined as the date halfway between the date of minimum EVI and the fastest greening date (Fig. 2B). Similarly, the date for the end of the greening season (EGS) is defined as the date halfway between the fastest brown-down date and minimum EVI date after a growing season. The peak (PGS) is defined as the date of maximum EVI during the growing season, and the length of the greening season (LGS) is the difference between EGS and SGS dates.

2.4. Meteorological and eddy covariance data

Gridded 0.05° resolution daily rain gauge precipitation data interpolated from ground station measurements were obtained from the

National Climate Center, Australian Bureau of Meteorology (Jones, Wang, & Fawcett, 2009) and were used to investigate the relationship between rainfall and spatio-temporal patterns in vegetation phenology. We used three flux towers along the NATT to analyze and interpret the satellite-derived measures of greening season activity. These sites were located at Howard Springs (12.495°S, 131.150°E) (Hutley & Beringer, 2011), Daly River (14.159°S, 131.383°E) (Beringer, Hacker, et al., 2011; Beringer, Hutley, Hacker, Neininger, & Paw, 2011), and Ti Tree (22.283°S, 133.249°E) (Eamus, Boulain, etal., 2013; Eamus, Cleverly, et al., 2013), representing the two most common savanna vegetation classes present in Australia: *Eucalypt* woodland and *Acacia* woodland (Table 1). The original Level 3 data were provided by the OZFLUX network (http://www.ozflux.org.au) and data preprocessing was used to ensure consistency among sites and reduce the uncertainties in computed fluxes; this included general quality control assessment, removal of outliers, and correction for low turbulence periods. A second-order Fourier regression was fitted to the nighttime Net Ecosystem Exchange (NEE) series, which is assumed to be a representative of Ecosystem Respiration (*Reco*), using the method proposed by Richardson and Hollinger (2005):

$$R_{eco} = f_0 = s_1 \times \sin(D_\pi) + c_1 \times \cos(D_\pi) + s_2 \times \sin(2 \times D_\pi) + C_2 \times \cos(2 \times D_\pi) + \varepsilon \tag{3}$$

where in Eq. (3), *f*0, *s*1, *c*1, *s*2 and *c*2 are fitted coefficients, $D\pi = DOY * 360/365$ (DOY: Day of Year), and ε is the regression residuals. We used this method because it had the advantage of minimal use of environmental covariates to compute *Reco* (Richardson & Hollinger, 2005). Half-hourly fluxes of Gross Ecosystem Productivity (GEP) were then derived as $GEP = NEE - Reco$.

As the intent of this study was to obtain a reliable time series of *GEP* observations in order to confirm MODIS satellite retrieved phenology metrics, we aggregated the half hourly flux data to match the 16-day temporal resolution of the MODIS EVI observations.

2.5. Spatial and temporal analysis sampling

We analyzed the spatial–temporal dynamics in phenology across our study area through the use of local site analyses, latitudinal transect analyses, and whole region spatial analyses (Fig. 1). The latitudinal transects pass through the major vegetation classes and include the local study sites and major field sites of the NATT (Hutley et al., 2011). The transect consisted of one hundred 0.05° × 0.05°samples, from 12.495°S–131.15°S to 22.283°S–133.353°S. Within this transect, phenological metrics were extracted for each year and for each sample to investigate latitudinal gradients in phenology along the NATT. Data processing, statistical analysis and visualization were conducted in R scientific computation environment (version 2.15.3, R Core Team, 2013).

3. Results

3.1. Local site phenological profiles

Seasonal EVI profiles (SSA reconstructed) with key phenology transition dates during the wettest and driest years over the six local study sites are depicted in Fig. 3. The seasonal EVI profiles varied in magnitude and timing of the key phenology dates, with the more tree-covered northern mesic sites (Howard Springs, Adelaide River, and Daly River) showing the highest amplitude EVI profiles (Fig. 3), and the southern drier *Acacia* woodland site (Ti-Tree) with the lowest overall EVI profiles (Fig. 3A, B). The seasonal profiles for the tussock grassland site (Sturt Plains), the mostly non-savanna area near the center of the transect, were also low in amplitude, particularly in dry years (Fig. 3B). The magnitude of peak greening season (PGS) values decreased along the rainfall gradient from north to south. Similarly, dry season minimum EVI values, prior to the start of greening season (SGS), also decreased in magnitude from north to south, reflecting a declining contribution from evergreen tree and shrub cover, as there is no green herbaceous presence during this late dry season period. Area-integrated integrals of the EVI curves also decreased from north to south indicative of the lower annual vegetation productivity across the savanna vegetation classes from northern *Eucalyptus* woodlands to the *Acacia* woodlands and grasslands to the south (Fig. 3).

Differences in phenology timing dates between northern mesic savanna classes to the southern xeric classes approximately followed the progression of the Australian summer monsoon (Fig. 3). On average, the start of greening occurred earlier in the north and was progressively delayed to the south, with SGS dates ranging from September to November, respectively. Similarly, the dates of peak greenness (PGS) and the end of the greening season (EGS) occurred earlier in the north and later into the south, lagging from January to April, and May to August, respectively.

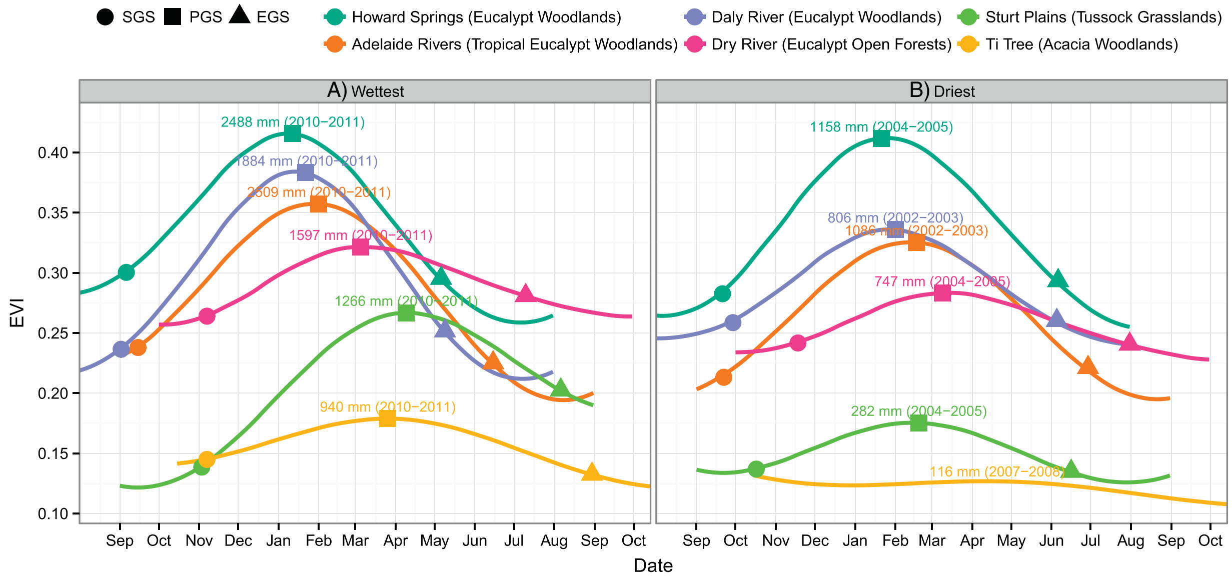

Fig. 3. Phenological profiles for 6 flux tower sites from 2000 to 2012. “Wettest” means the seasonal EVI profile from the wettest year (with the highest annual precipitation) and “driest” means the profile from the driest year (with the lowest annual precipitation) during 2000–2012, for each site. SSA derived key phenology transitional dates, annual precipitation and hydrological year have also been labeled for each site.

Hydroclimatic differences in EVI seasonal profiles and phenological transition dates between the wettest year and driest years were also evident (Fig. 3). The wettest year for all six sites was 2010–11, a La Niña year, while the driest years were 200203 (Adelaide River, Daly River), 2004–05 (Howard Springs, Dry River, Sturt Plains) and 2007–08 (Ti Tree). During the driest years, the northern *Eucalyptus* forest/woodland sites (Howard Springs, Adelaide River, Daly River and Dry River) showed delayed trends in SGS, PGS and EGS from 5 to 30 days, relative to wet years. The drought year influence on phenology was more complex at the two southernmost sites, where the Ti Tree site had no detectable greening season at all, and the non-savanna Sturt Plains site showed an earlier, although considerable smaller, greening season (Fig. 3A, B). Overall, the impacts of changing rainfall amounts on the seasonal EVI profiles became more strongly felt from north to south along the transect. Changes were minimal at the mesic savanna site (Howard Springs), despite the considerable reduction in annual precipitation from 2488 mm to 1158 mm (Fig. 3). This suggested a more energy-limited, rather than water-limited savanna class. In contrast, at the southern xeric end, seasonal EVI amplitudes decreased from 0.27 to 0.18 in tussock grasslands (~33% decrease), and dropped by 73% at the Ti Tree site *Acacia* woodland.

3.2. Phenogram

The inter-annual variations in the key phenological events are shown in Fig. 4 for the same sites and major vegetation assemblages. Inter-annual variations in phenology at the Eucalypt woodland and tropical Eucalypt woodland sites (Howard Springs, Adelaide River, and Daly River) were minimal, although there appears to be an advancing trend in SGS, PGS, and EGS at Howard Springs and Daly River sites in the last 5 years, from 2006–07 to 2011–12 (Fig. 4A, C). Increases in inter-annual variability in phenology became apparent at the Eucalypt open forest (Dry River) site, and became quite pronounced in the tussock grassland (Sturt Plain) and *Acacia* woodland sites

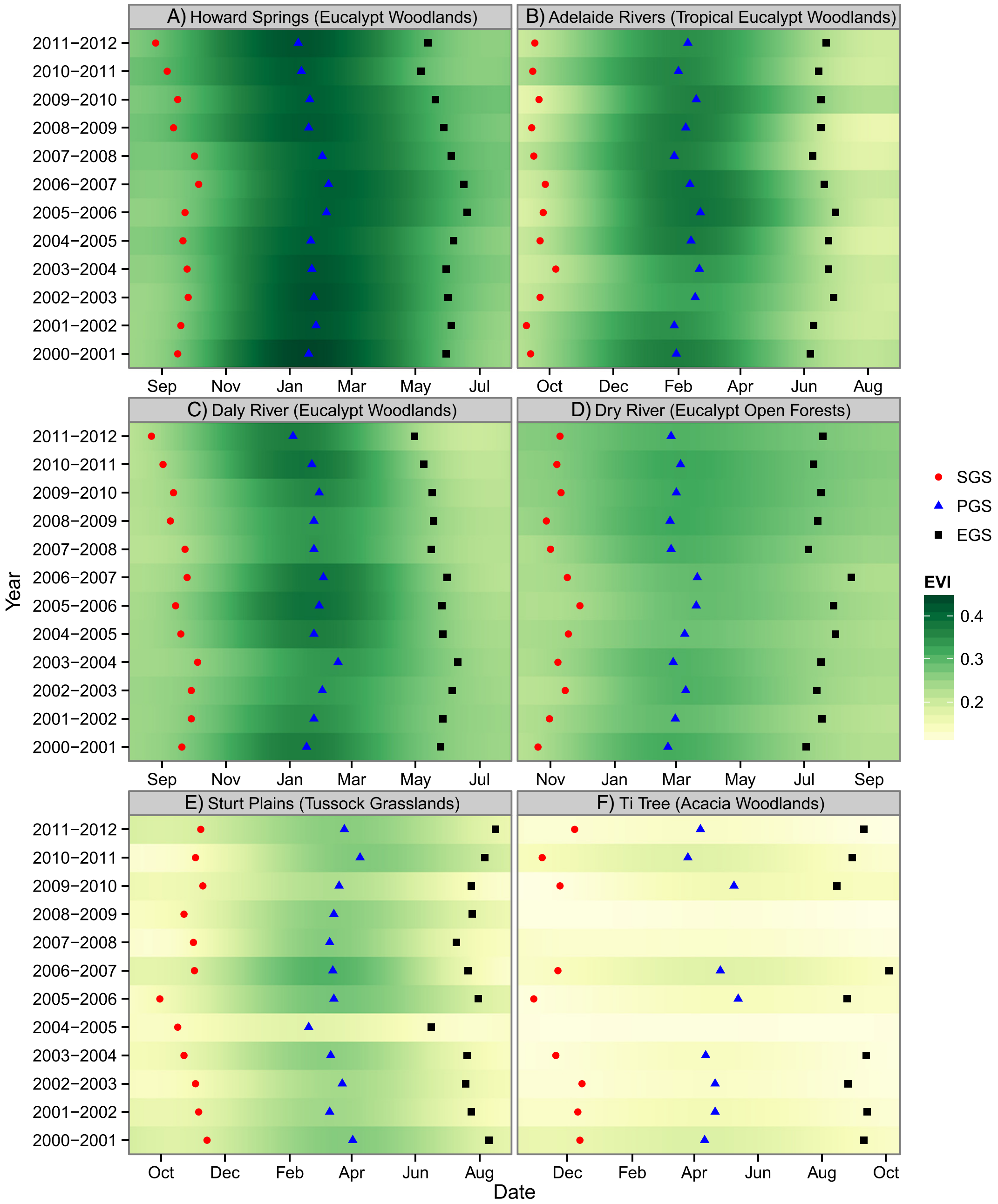

Fig. 4. Phenogram–inter-annual variations in vegetation phenology plotted with intra-annual EVI seasonality as background for six major sites from 2000 to 2012.

(Ti Tree) (Fig. 4D, E, F). The extreme regional drought in 2004–05 resulted in dramatic and earlier advances in PGS, EGS, and subsequent year SGS of 1 month at Sturt Plains, and the absence of a detectable greening season at Ti Tree. The Ti Tree site also lacked a greening season in 2007–08 and 2008–09 due to severe drought conditions (Fig. 4F).

3.3. Towards a realistic representation of xeric vegetation phenology

Subtle variations in EVI values in low rainfall areas with low greenness may not necessarily depict true vegetation growth dynamics, due to the influence of noise in the satellite data associated with bidirectional sun/viewing angles and residual atmosphere aerosol and clouds (Wang et al., 2012; Glenn et al., 2008). To minimize potential artifacts in our retrievals, we applied a seasonal amplitude threshold value of 0.02 EVI units as our objective criteria of MODIS uncertainties in the data, and defining our basis for phenology detection. In Fig. 5, the EVI seasonal amplitude (peak minus baseline) is plotted against annual precipitation over the 13 year time period at the driest, Ti Tree site. EVI amplitudes varied widely from 0.005 (2004–05) to 0.060 (2006–07), while rainfall varied from 116 mm to 940 mm, i.e., both varied approximately ten-fold. The resulting strongly significant positive correlation ($R = 0.83$, $p < 0.001$) suggests that variations in seasonal EVI may reflect actual vegetation dynamics driven by inter-annual variations in rainfall. Nevertheless, at annual precipitation values below ~250 mm, the EVI seasonal amplitude drops below 0.02 EVI units, which is within the mean uncertainty of the MODIS EVI product, and hence all pixel-years with EVI seasonal amplitudes lower than 0.02 were excluded from phenology retrievals, and treated as 'null' values with no detectable greening seasons.

3.4. Biogeographic patterns of phenology

Region-wide phenology maps were generated to assess spatial variability and inter-annual variability in the timing and length of seasonal greening over the NATT study area (Fig. 6). Four individual years are depicted to illustrate the impacts of inter-annual rainfall variability on vegetation phenology, including a relatively normal rainfall year (2001–02), an anomalous drought year (2007–08), and two relatively wet years (2005–06 and 2010–11), based on the standard precipitation anomalies (Fig. 6A). Large spatial variations in the timing and occurrence of key phenology transition dates are readily observed over the study area (Fig. 6B, C, D). There is an overall delaying trend in SGS, PGS, and EGS from north to south with the greening season starting earlier (between September and October) at the northern, mesic *Eucalyptus*-dominated forests and woodlands, followed by gradual delays to November and the subsequent February towards the southern hummock grasslands and *Acacia*-dominated savannas (Fig. 6B). The peak and end date of greening season (PGS and EGS) showed similar, delayed trends from north to south, and shifted from January to May, and June to December, respectively (Fig. 6C, D).

Large temporal variations in annual precipitation primarily impacted vegetation growth in the southern region (*Acacia*-dominated savannas and hummock grasslands) with the northern humid regions (*Eucalyptus*-dominated savannas) more buffered to rainfall variability (Fig. 6B, C, D, E).

Patterns in the length of greening season (LGS) were more complex, especially in the southern xeric areas where in some years a longer greening season was observed relative to the northern savannas, while in drought years depressed vegetation activity was particularly evident in the south, such that no detectable LGS was observed (Fig. 6E).

The latitudinal changes in phenology were more easily depicted in the 1100 km transect plot (one hundred pixels, 0.05° × 0.05°) from Howard Springs to Ti-Tree for dry and wet years (Fig. 7). Well-defined latitudinal delayed shifts in SGS, PGS, and EGS were observed over the northern half of the transect from 12.5°S to 17.7°S, which is the approximate geographical boundary separating the northern mesic *Eucalyptus* dominated forests/woodlands from the xeric *Acacia* woodlands/shrublands and the hummock grasslands in the southern portion of the study area (Fig. 7A). The SGS date varied from September in the northern end of the transect to November at 17.7°S, after which the delaying trend was replaced by a more fluctuating and variable pattern with slight advancing trends in the southernmost portion of the transect (Fig. 7A).

Phenology shifts in PGS and EGS followed similar latitudinal trends, with PGS dates delayed from late January to late March and EGS dates deferred from late May to early September from north to south (Fig. 7A). The peak greening seasonal period (PGS) and end of the greening season (EGS) also showed much higher latitudinal variability and followed an advancing trend south of 17.7°S. Overall, the length of the greening period was relatively stable throughout the northern savannas, and became highly variable south of 15.5°S, where LGS duration became shorter or longer than LGS of the northern savannas (Fig. 7B). Note that, despite the global spatial trends observed along the 1100 km transect, there were also local fluctuations present, related to local-environmental controls (such as topography, soil type, rainfall patterns), and vegetation structure and species composition.

In comparisons of the wet and dry years along the 1100 km transect, the phenology of the mesic savannas at the northern end of the transect was stable and consistent across the wet and dry years, indicating that greening periods (duration and dates) were relatively insensitive to inter-annual variability in rainfall amount. The SGS, PGS, and EGS parameters were fairly constant across dry and wet years, resulting in a relatively constant LGS (Fig. 7B). However in the southern end of the transect study area, the impact of dry and wet rainfall years became more pronounced, particularly for the start of greening season (SGS) in which significant advances in greening occurred in wet years while large delays in SGS were observed in the dry years (Fig. 7A). SGS sensitivity to dry and wet years was maximal between 17°S and 21°S (with a maximum difference of 46 days found at 18.3°S), which approximately corresponded to the geographical extent of hummock grasslands. On the other hand, PGS and EGS dates were much more stable across years regardless of rainfall amounts (Fig. 7A).

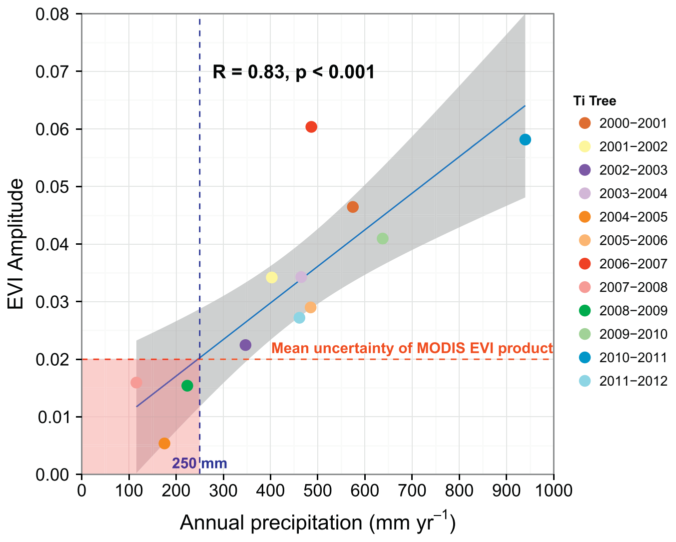

Fig. 5. Relationship between annual precipitation and EVI season amplitude (peak-baseline) for the south arid endmember of NATT, Ti Tree (*Acacia* woodlands), over 2000–2012 period. Horizontal red dashed line indicates the mean uncertainty of MODIS EVI product (0.02 EVI unit). Vertical blue dashed line indicates the minimal requirements of annual rainfall for reliable phenology detection at Ti Tree site. Red shaded area indicates the low annual rainfall region with EVI seasonal amplitudes lower than MODIS data error such that reliable phenology could not be retrieved.

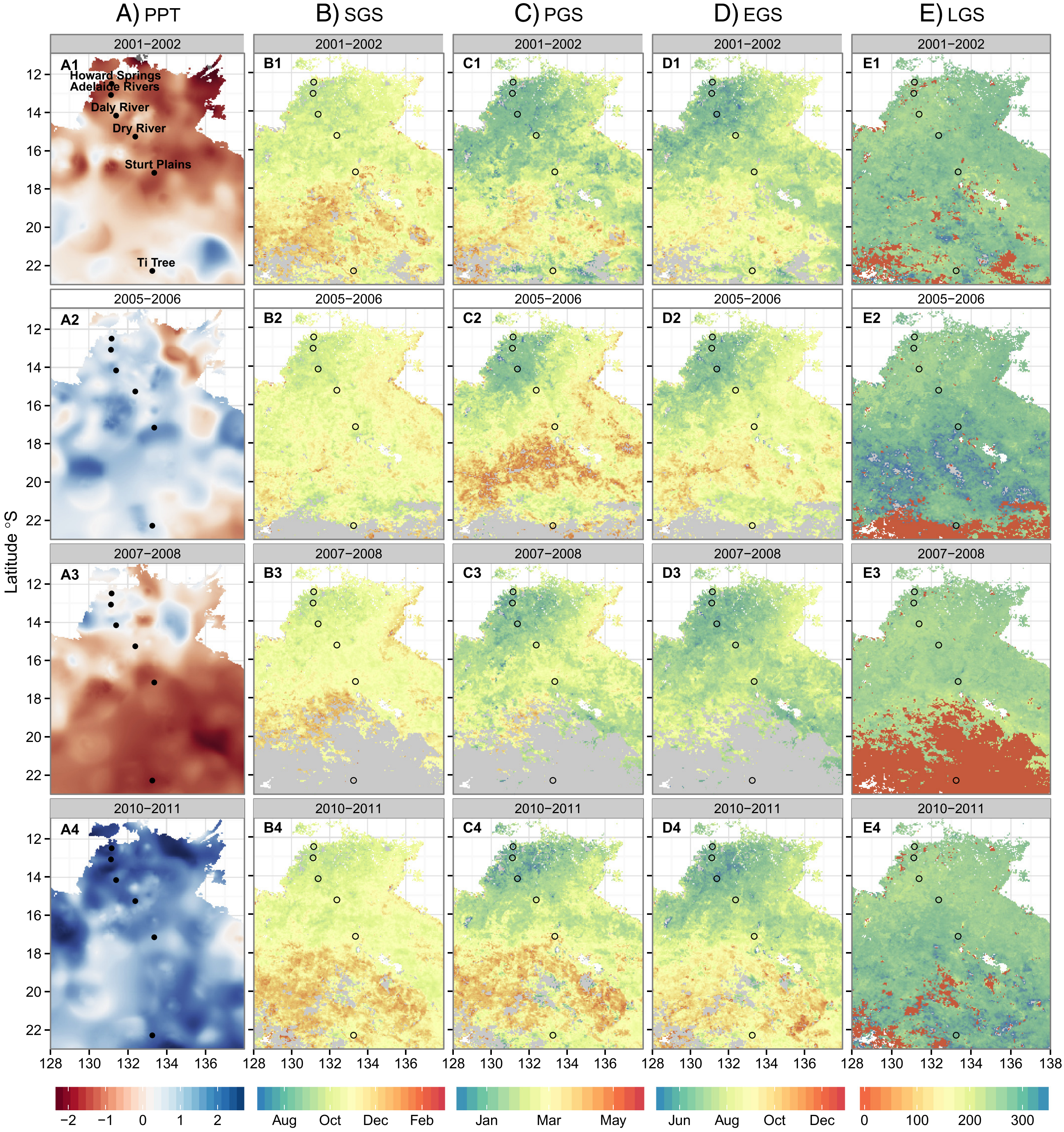

Fig. 6. Spatial patterns of vegetation phenology over the NATT study area along with rainfall anomalies across four representative hydrological years. (A) Standardized anomaly of annual precipitation; (B) Start of Greening Season (SGS); (C) Peak of Greening Season (PGS); (D) End of Greening Season (EGS); (E) Length of Greening Season (LGS). Four representative years we selected were: 2001–2002 (normal/light drought year); 2005–2006 (wet year); 2007–2008 (drought year); 2010–2011 (wet year). The filled pixels (gray shaded areas) are either water body, low MODIS QA, or without detectable phenology.

During the wetter years, LGS ranged between 240 and 280 days across most of the northern portion of the transect (from 12°S to 15.5°S), which continued or increased in the southern portion of the transect to around 300 days until 17.7°S, then kept decreasing to 280 days towards the south end (Fig. 7B). In contrast, during the drier years, there were dramatic declines in LGS in the mid-south portion of the transect (from 15.5°S to 19°S), with significant areas in which no detectable greening season could be reliably assessed (Fig. 7B).

3.5. Phenology and precipitation averaged by vegetation groups

To examine co-varying influences of rainfall and savanna vegetation class on observed phenology along the ecological rainfall transect, we plotted the inter-annual variability observed in LGS with the mean and variance in rainfall for all pixels within each of the nine major vegetation groups in the study area (Fig. 8). We observed, a strong negative relationship between inter-annual variance in LGS and mean annual

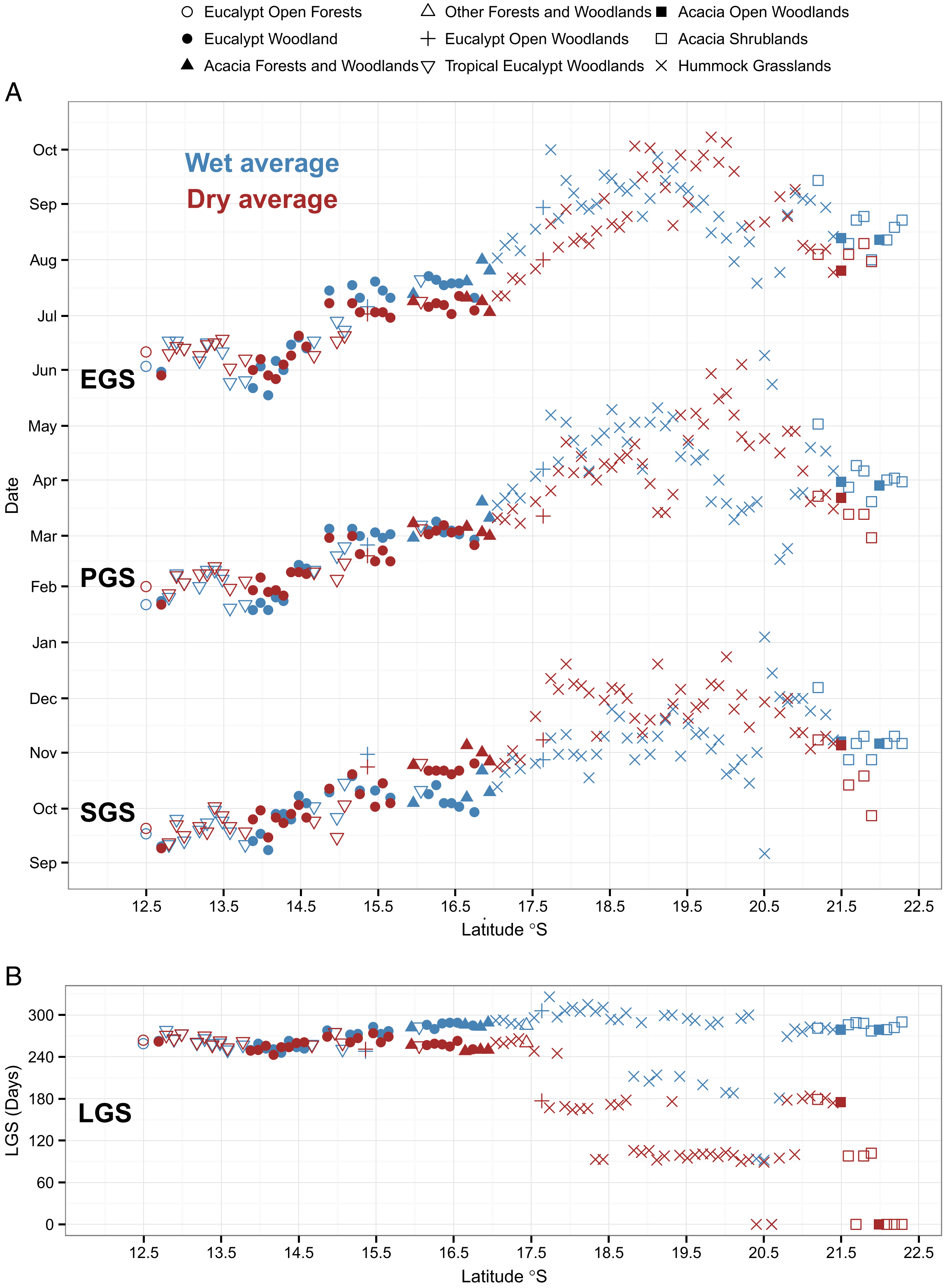

Fig. 7. Latitudinal gradients of vegetation phenology along the NATT from 12.5°S to 22.5°S. For each transect sample, to produce the wet average and dry average, we first ranked the 12 years based on annual precipitation and then averaged the phenological metrics of the three wettest years and three driest years to form "wet average" and "dry average".

precipitation (MAP) with very low LGS variance in the humid areas and increasing LGS variance towards the southern xeric vegetated areas (Fig. 8A). This increasing variance in LGS coincided with the transition of vegetation groups from tropical Eucalypt forest/woodlands, tussock grasslands, *Acacia* forests/woodlands, and Eucalypt open woodlands to hummock grasslands, *Acacia* open woodlands, and *Acacia* shrublands (Fig. 8A). The two most humid vegetation classes, Eucalypt open forests (MAP = 1391 mm) and tropical Eucalypt woodlands (MAP = 1311 mm), exhibited the smallest temporal variations in LGS (5.2% and 5%, respectively). The largest variation in LGS occurred over

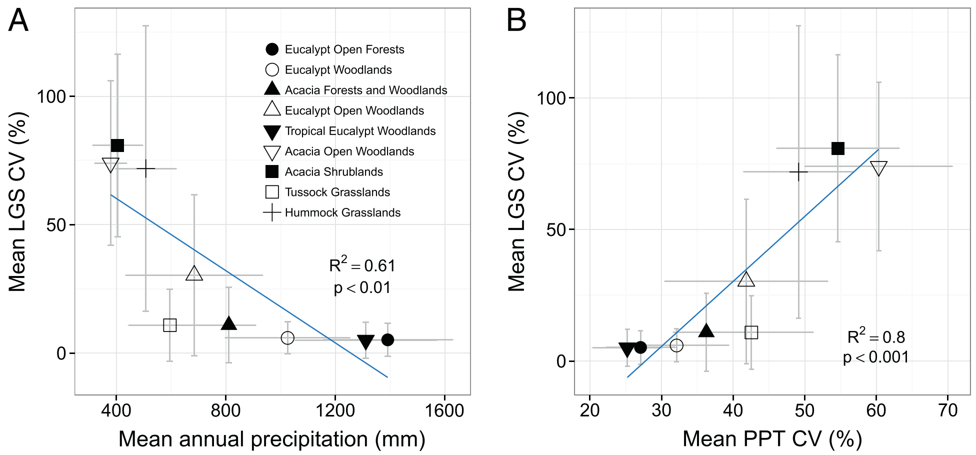

Fig. 8. Regional averaged (A) mean CV (coefficient of variance, %) of length of greening season (LGS) versus mean annual precipitation (PPT), and (B) mean CV of LGS versus mean CV of PPT for nine major vegetation groups.

the *Acacia* shrublands (80.9%), open woodlands (74%) and hummock grasslands (71.9%), where MAP was 405 mm, 379 mm and 508 mm, respectively.

There was a strong positive correlation ($R^2 = 0.8$, $p < 0.001$) between inter-annual variances in precipitation and variance in LGS (Fig. 8B). Variance in LGS showed a slow increase with increasing variance in annual precipitation up to CV-PPT values of 40% followed by a rapid increase in LGS variability at higher CV-PPT up to a maximum CV-LGS of 81% variance at values of CV-PPT that exceeded 55% (Fig. 8B). The increasing trend in LGS variability followed changes in vegetation structure, from dense tree cover classes (Eucalypt tropical forest/woodlands) to lower tree cover (*Acacia* shrublands, open woodlands, and hummock grasslands) (Fig. 8).

3.6. Eddy covariance flux measurements of photosynthesis

We compared the seasonal synchronies of the MODIS EVI retrieved phenological timing events with in-situ flux tower measurements of photosynthetic activity to independently assess our satellite phenology retrieval methodology (Fig. 9). Overall, the seasonality of 16-day aggregated GEP was consistent with the MODIS EVI time series at the Howard Springs and Daly River sites with good correspondence in retrievals of phenological transition dates (Fig. 9 and Table 3). At Howard Springs site, the RMSE between MODIS EVI retrieved phenology dates and flux tower GEP based phenology were 12.2, 9.5, 11.1 and 13.8 days for SGS, PGS, EGS and LGS, respectively (Fig. 9A and Table 3). At Daly River site there was a relatively higher RMSE between the EVI and GEP-based metrics (19.1, 10, 20.8 and 19.8 days for SGS, PGS, EGS and LGS, respectively), although large gaps in the tower GEP time series contributed to the higher uncertainties (Fig. 9C and Table 3). The EVI-derived seasonal peak date (PGS) lagged the flux tower derived PGS, indicating that peak photosynthesis activity precedes the appearance of the chlorophyll-based, EVI greenness signal (Fig. 9C).

The highly variable Ti Tree site also showed a good seasonal correspondence of photosynthesis with satellite-derived greening periods (Fig. 9D). Most importantly, the GEP seasonal profiles confirm the extended greening season periods in the semi-arid southern *Acacia* woodland savannas. This site also demonstrated the highest uncertainty in capturing flux tower GEP seasonal dynamics with the satellite phenology measures. MODIS and flux tower PGS were generally consistent in both years, however, MODIS PGS lagged tower-GEP by approximately 3 weeks (Fig. 9D and Table 4). The uncertainties in SGS and EGS between the two datasets were greater, particularly in estimating the end of the greening season with MODIS EVI lagging GEP by as much as 3 months.

Uncertainties in SGS and EGS can be partly explained by observed hysteresis effects between greening (SGS to PGS) and browning (PGS to EGS) phenological phases in MODIS EVI and flux tower GEP (Fig. 10). The green-up and brown-down phase relationships between MODIS EVI and flux tower GEP at Howard Springs were in close agreement with near-linear relationships and similar slopes (Fig. 10A). Differences in these relationships became greater at the Daly River site, with green-up and brown-down relationships showing different slopes and some non-linearity evident in the brown-down phase (Fig. 10B). The largest differences between the two phases were observed at the Ti Tree Mulga site, with the brown-down phase showing clear non-linear relationships between MODIS EVI and flux tower GEP (Fig. 10C). This corresponded with the greater uncertainties found in defining the end of the greening season dates.

4. Discussion

4.1. Ground interpretations of the remotely sensed vegetation phenology

In this study we characterized the biogeographical variability in landscape phenology over a wide range of tropical savanna vegetation classes (tree-shrub-grass assemblages) along a tropical mesic to semi-arid rainfall gradient with 13 years of MODIS EVI data and a Singular Spectrum Analysis (SSA) based algorithm for retrieval of phenology dates. Before discussing our results, we first provide ground interpretations of the remotely sensed vegetation phenology in north Australian tropical savannas. We assumed that seasonal variations (phenology) in EVI should be primarily the result of changes in plant cover associated with changes in understorey grasses and forbs. We support this assumption through consideration of the following:

1. Field observations of leaf phenology of woody species (trees and tall shrubs) at sites located at the north end of the NATT (Solar Village, near Darwin, Northern Territory, Australia and Howard Springs, near Darwin) showed that evergreen species expressed only small seasonal fluctuations in LAI with a full canopy retained throughout the year (O'Grady, Chen, Eamus, & Hutley, 2000; Williams et al., 1997). This is attributable to their ability to access deep soil stores of water and ground water (Borchert, 1994; Cook et al., 1998). The two community dominants, *Eucalyptus miniata* and *Eucalyptus tetrodonta*, account for approximately 80% of the standing tree biomass, and are responsible for overall high projected canopy foliage during the dry season (Duff et al., 1997; Williams et al., 1997; O'Grady et al., 2000);
2. An EC flux tower based study located at Howard Springs showed that tall grasses and shrubs contributed 70–80% of total ecosystem carbon

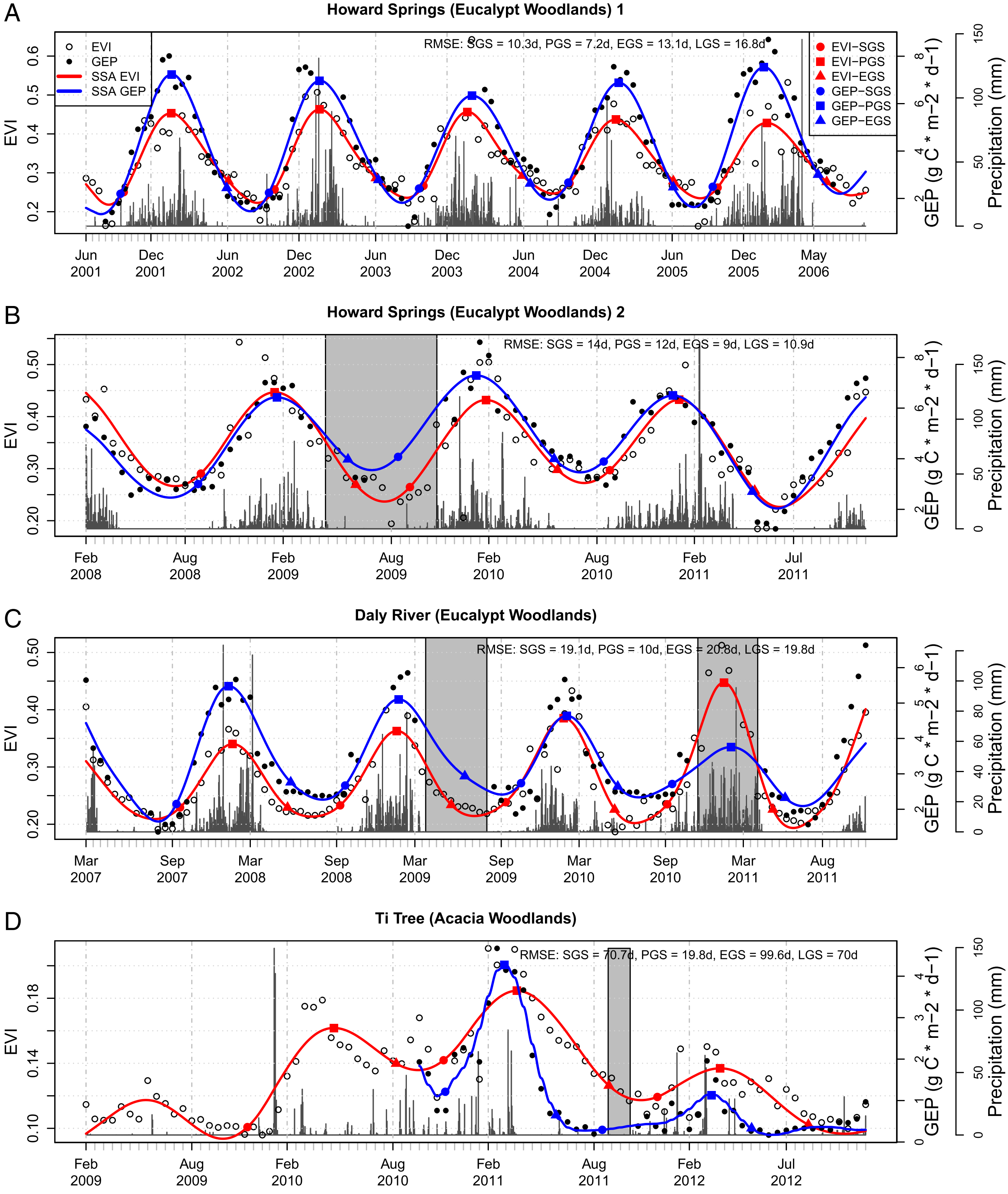

Fig. 9. Inter-comparison of the MODIS EVI time series and flux tower GEP time series over three local sites. (A) Howard Springs (2001–2006); (B) Howard Springs (2008–2011); (C) Daly River (2007–2011); (D) Ti Tree (2009–2012). Phenology metrics computed for both EVI and GEP using same algorithm. Shaded areas indicate time periods which have continuous missing gaps presented in flux GEP data. These missing gaps were filled using linear interpolation and then used to calculate phenology metrics.

fluxes during the wet season but contributed zero in the mid-to-late dry season (Whitley et al., 2011), but transpiration rates of the trees were found to be constant across wet and dry season (Hutley et al., 2001);

3. At the southern semi-arid region of the NATT, field measurements in the *Acacia* dominated woodlands (Ti Tree) found that *Acacia aneura* (evergreen) shows only small variation in Leaf Area Index (LAI) (Eamus, Boulain, et al., 2013; Eamus, Cleverly, et al. 2013). They found that variations in ecosystem leaf area index were primarily contributed by the understorey, which peaked during the wet season (0.3) and were minimal in the dry season (0.05), therefore the variations in understorey LAI were assumed to be the predominant driver of seasonal changes in canopy gas exchange at this Mulga site (Eamus, Boulain, et al. 2013; Eamus, Cleverly, et al., 2013).

Table 3
Phenological metrics calculated using MODIS EVI and flux GEP for Howard Springs.

Pheno-metrics	Data	Hydrological year							
		2001–2002	2002–2003	2003–2004	2004–2005	2005–2006	2008–2009	2009–2010	2010–2011
SGS	GEP	2011.09.19	2002.09.20	2003.09.25	2004.09.27	2005.09.18	2008.09.04	2009.08.25	2010.08.25
	EVI	2011.09.27 (+8)[a]	2002.10.04 (+14)	2003.10.06 (+11)	2004.09.30 (+3)	2005.09.30 (+12)	2008.09.09 (+5)	2009.09.15 (+21)	2010.09.05 (+11)
PGS	GEP	2002.01.23	2003.01.23	2004.02.03	2005.01.29	2006.01.22	2009.01.22	2009.01.11	2010.12.26
	EVI	2002.01.22 (−1)	2003.01.23 (0)	2004.01.22 (−12)	2005.01.22 (−7)	2006.01.30 (+8)	2009.01.18 (−4)	2010.01.28 (+17)	2011.01.06 (+11)
EGS	GEP	2002.06.08	2003.06.17	2004.06.25	2005.06.13	2006.06.05	2009.05.28	2010.05.29	2011.05.16
	EVI	2002.06.12 (+4)	2003.06.11 (−6)	2004.06.06 (−15)	2005.06.13 (0)	2006.06.26 (+21)	2009.06.11 (+14)	2010.06.04 (+6)	2011.05.20 (+4)
LGS	GEP	262	270	274	259	260	266	277	264
	EVI	258 (−4)	250 (−20)	244 (−30)	256 (−3)	269 (+9)	275 (+9)	262 (−15)	257 (−7)

[a] Number within the bracket represents the difference between the phenological metrics (date or length) calculated using EVI and GEP. Taking SGS_{EVI} and SGS_{GEP} for example, if it is a positive number, it means that SGS calculated using EVI delayed the SGS calculated using GEP, and vice versa.

Based on these observations it is clear that the primary determinant of the green-up and brown-down is defined primarily by the dynamics of the understorey grasses and forbs, with a *relatively* invariant evergreen-dominant tree seasonality. However, we also note that the woody species, despite primarily dominated by evergreen species, also contribute to seasonal variations in EVI/flux because there are some deciduous, semi-deciduous and brevi-deciduous trees present in the northern mesic region of the NATT (Williams et al., 1997). Similarly at Ti Tree in the southern region of the NATT, variation in LAI of the Mulga (*A. aneura*) ranged from 0.2 to 0.3 (Eamus, Boulain, et al. 2013; Eamus, Cleverly, et al., 2013).

In this study, we focused on the timing of functional phenology patterns at landscape scales, rather than partitioned physiognomic landscape components. However, we acknowledge that it would be worthwhile to decompose the EVI greenness signal into tree, grass, and shrub contributions and further retrieve phenological metrics for each layer. To date such physiognomic partitioning has not been accomplished by remote sensing observations at regional scales; nor has such partitioning been accomplished with flux tower measurements at community scales. Therefore, this should be a common goal and research challenge for both remote sensing and eddy flux communities in future savanna research. For example, Guerschman et al. (2009) attempted to improve the partition of photosynthetic vegetation, non-photosynthetic vegetation and bare soil by incorporation of a shortwave infrared (SWIR) band. Unique phenological characteristics between woody species and herbaceous species in Australian savannas have also been recognized and used for obtaining sub-pixel tree/grass partitions (Donohue et al., 2009; Lu et al., 2003; Roderick et al., 1999). Such partitions will benefit many scientific research and applications such as forage resource management, hydrological cycle simulation, fire fuel loading and modeling carbon and water exchanges between land surface and atmosphere.

4.2. Biogeographical patterns of vegetation phenology

Significant latitudinal shifts in vegetation phenology timing throughout the northern half of the study area (from 12°S to approximately 17.7°S) were observed, coincident with the extent of the monsoonal rainfall (Bowman et al., 1988). The start, peak, and end dates of the seasonal greening periods were progressively delayed from north to south, resulting in a relatively constant duration of the green season period despite the large rainfall gradient of 1700 mm to 700 mm mean annual rainfall for this northern portion of the transect. We also observed an increasing trend in inter-annual variability of the timing of key phenology dates from the northern mesic Eucalypt savannas to the southern semi-arid *Acacia* savanna woodlands and grasslands. This followed a progressively weakening influence of monsoon activity towards the southern *Acacia* woodlands where more isolated convective storms with large inter-annual variability become more dominant climatic influences (Cook & Heerdegen, 2001).

The main determining factor of phenology in the northern mesic tropical Eucalypt savannas is the timing of the onset of the monsoonal rainy season, a response that is primarily attributed to the growth of grasses that are limited by soil water availability. The low inter-annual variability observed in phenological patterns in the northern savannas was related to the low inter-annual variability in the timing of the onset date of the rainy season (standard deviation of approximately 10 days) (Lo et al., 2007). Large inter-annual variations in precipitation amounts had no observable effects on phenology timing in the northern savannas, as the duration of rainy season is not related to the amount of rainfall (Cook et al., 1998) and hence phenology was largely decoupled from variability in the amount of precipitation.

In contrast to the northern savannas where duration of the rainy season played a more important role than rainfall amount in dictating seasonal growth, phenology was strongly coupled to the absolute

Table 4
Phenological metrics calculated using MODIS EVI and flux GEP for Daly River and Ti Tree.

Pheno-metrics	Data	Daly River				Ti tree	
		2007–2008	2008–2009	2009–2010	2010–2011	2010–2011	2011–2012
SGS	GEP	2007.09.23	2008.10.02	2009.10.28	2010.09.29	2010.11.16	2011.08.28
	EVI	2007.10.01 (+8)[a]	2008.09.21 (−11)	2009.09.24 (−34)	2010.09.18 (−11)	2010.11.13 (−3)	2011.12.06 (+100)
PGS	GEP	2008.01.17	2009.01.29	2010.02.07	2011.02.07	2011.03.03	2012.03.13
	EVI	2008.01.26 (+9)	2009.01.25 (−4)	2010.01.31 (−7)	2011.01.22 (−16)	2011.03.26 (+23)	2012.03.31 (+16)
EGS	GEP	2008.06.03	2009.06.25	2010.05.31	2011.06.07	2011.06.05	2012.05.25
	EVI	2008.05.27 (−7)	2009.05.26 (−30)	2010.05.24 (−7)	2011.05.11 (−27)	2011.09.09 (+96)	2012.09.05 (+103)
LGS	GEP	254	266	215	251	201	271
	EVI	239 (−15)	247 (−19)	242 (+27)	235 (−16)	300 (+99)	283 (+3)

[a] Number within the bracket represents the difference between the phenological metrics (date or length) calculated using EVI and GEP. Taking SGS_{EVI} and SGS_{GEP} for example, if it is a positive number, it means that SGS calculated using EVI delayed the SGS calculated using GEP, vice verse.

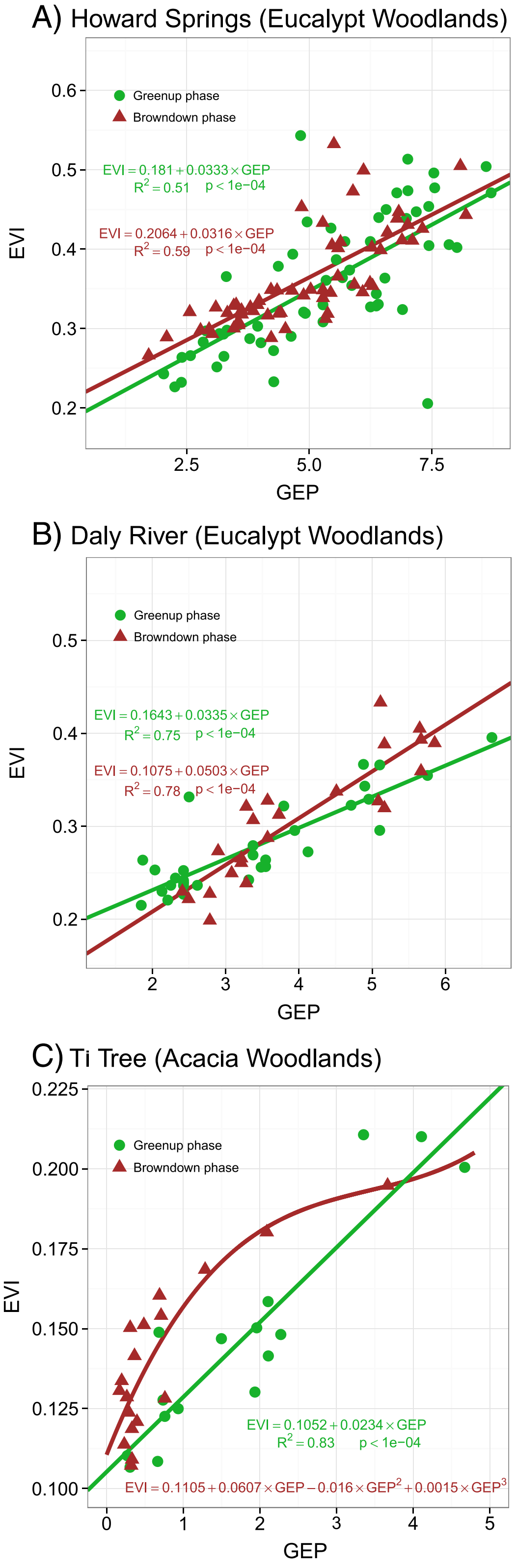

Fig. 10. Scatter plot between 16-day aggregated flux tower GEP and MODIS 16-day EVI for three savanna sites. (A) Howard Springs (Eucalypt woodlands); (B) Daly River (Eucalypt woodlands) and (C) Ti Tree (*Acacia* woodlands). Seasonal hysteresis effect in the relationship between EVI and GEP was found maximum at Ti Tree Mulga site, while the greenup phase showed near-linear relationship, but browndown phase showed enhanced non-linearity. Greenup phase was defined as the period from season start (SGS) to season peak (PGS), while browndown phase was defined as the period from PGS to season end (EGS).

amount of rainfall in the southern semi-arid areas (i.e. south of 15°S, the southern limit of monsoonal tall-grass savannas). The relative contribution of temporally isolated extra-monsoonal rainfall events to both the duration of the rainy season and the amount of rainfall increases toward the south and is considered a critical determinant of many important ecological processes such as seed germination of grasses and woody species phenology (Eamus et al., 2001). Additionally, inter-annual variability of start and end dates of the rainy season length was much greater in the southern region, where the standard deviation in the timing of onset of rainfall exceeded 55 days (Lo et al., 2007) and coincided with increased variation in phenology along the same direction. Therefore, rainfall was more important for regulating phenology over the semi-arid southern study area, thereby stimulating seed germination of the herbaceous species and defining the length of the seasonal green period (Fox, 1990).

4.3. Ground GEP comparisons

Seasonal in-situ eddy covariance flux measurements of GEP were used to assess how well coarse resolution MODIS satellite observations of vegetation greenness and retrieved phenology compared with ground measurements of photosynthesis in savanna landscapes. Such comparisons of flux data with remote sensing studies of phenology have rarely been undertaken. MODIS EVI, as a spectral greenness index, was strongly correlated to tower GEP fluxes at three tower sites representing two contrasting savanna vegetation classes: *Eucalyptus* dominated woodlands and *Acacia* dominated woodlands, along a gradient in mean annual precipitation from 1722 mm to 443 mm. The Pearson correlation coefficient (R) between MODIS EVI and tower GEP was 0.83, 0.9 and 0.83 for Howard Springs, Daly River and Ti Tree respectively (all $p < 0.001$).

The Ti Tree site was of particular interest because the observations at this site (since September 2010) enabled an independent assessment of the impacts of the 2010–2011 La-Nina event on vegetation functioning at this dry end of the NATT. Rainfall during this period was doubled the 13 year average (442 mm), and almost tripled the long term average (318 mm, 1981–2011) (Eamus, Boulain, et al. 2013; Eamus, Cleverly, et al., 2013). The GEP pulse (4.67 g C m^{-2} d^{-1}) was more than half of the maximal GEP (8.7 g C m^{-2} d^{-1}) at Howard Springs, demonstrating the enormous productivity potential of the Mulga savannas in central Australia. Most importantly, this GEP pulse was *independently* captured by both flux tower measurements and MODIS observations.

However, there were important differences in the relationships of MODIS EVI and flux tower GEP during the green-up versus the brown-down periods at the Ti Tree site. This "hysteresis effect" has been previously reported in other regions and is caused by the fact that declines in photosynthetic activity arising from low soil moisture content arise rapidly through stomatal closure but the loss of LAI and chlorophyll degradation are much slower processes (Huemmrich, Privette, Mukelabai, Myneni, & Knyazikhin, 2005; Jenkins et al., 2007). Hanan et al. (2002) suggested that "green" leaves seasonally vary in their photosynthetic capacity, and only the chlorophyll fraction of absorbed photosynthetically active radiation will drive GEP fluxes. Thus the discrepancies between EVI and GEP during the brown-down, senescence period may also be associated with the accumulation of non-photosynthetically-active materials of plants (e.g. litter and woody debris) (Asner, Wessman, & Archer, 1998).

We further note that determination of the minima in the EVI can be difficult and consequently establishing the end of a greening season may be difficult to assess under such conditions of gradual curing of grasses with only a gradual fading of the green color and an increasing accumulation of cured dry matter. Although not assessed in this study, the evergreen *Acacia* tree leaves may also undergo fluctuating and slowly decaying changes in leaf greenness, as it is known that evergreen trees may have periods of minimal functioning even though their leaves remain green in appearance (O'Grady et al., 2009).

In summary, we conclude from the rainfall and flux tower comparisons, that the MODIS EVI-based retrievals of phenology at Ti Tree and the other sites represent actual vegetation dynamics. Future studies are needed to further investigate the biophysical causes of differences between remotely sensed spectral indices and tower measurements of carbon/water fluxes. Such studies will not only benefit from better understanding of land surface phenology, but also facilitate the up-scaling of flux tower data with remote sensing, which results in better understanding of savanna ecosystem functioning and improved spatial modeling of biophysical parameters, productivity, and phenology.

4.4. Phenology and climate variability

Rainfall amount variability was a major environmental determinant of variability in vegetation phenology, especially within the intermediate and low rainfall regions of the NATT transect. Strong and non-linear relationships were observed between the CV of length of greening season (LGS) and both mean annual precipitation (PPT) and inter-annual precipitation variability (CV). Averaged by vegetation groups, the CV of annual precipitation alone could explain more than 80% of the variation encountered in LGS. However, an associated and co-varying factor that contributed to inter-annual phenologic variability was the relative ratio of woody versus herbaceous cover. Decreases in woody tree from the northern *Eucalyptus* to southern *Acacia*-dominated savanna classes were also associated with increasing variability in the timing of phenology events. Thus, decreases in total rainfall amount with increases in its variability toward the drier southern study areas are associated with lower overall tree/grass ratio and higher phenology variability.

In the semi-arid, southern end of the transect (MAP < 450 mm), storm driven rainfall distributions and the high frequency of low intensity rainfall events favor shallow rooted tree species that maximize rapid uptake of soil moisture, thereby allowing quick vegetation response to rainfall (Cook et al., 2002; Hutley et al., 2011). Greening patterns in this area are determined by the grass dynamics that are more dependent on rainfall to maintain ecosystem functioning, including seed germination. In contrast, the northern savannas, which have a higher tree/grass ratio, showed very little phenological variability, even across widely fluctuating inter-annual rainfall amounts. Further studies are needed to more critically evaluate the relative roles of tree/grass ratio and rainfall variability on controls of phenology.

Over the past 2–3 million years, the climate in north Australia has become more seasonal and fire prone, with *Eucalyptus* and *Corymbia* species evolving fire and drought tolerances (Bowman, Brown, et al., 2010; Bowman, Murphy, & Banfai, 2010). In the southern portion of our study area, hummock grasslands thrive over low-nutrient soils (Beard, 1981) and extremely variable amounts and timing of rainfall, thus capable of tolerating high levels of moisture stress (Griffin, 1984). The woody vegetation (*Acacia*) has adapted to the drying climate over the past 500 kyr (Martin, 2006; Morton et al., 1995), and the tolerance and adaptability of *Acacia* and spinifex species have prevented central Australia from becoming a desert. Thus, despite the large inter-annual variability of the timing of vegetation phenology over the southern areas, it is difficult to determine whether these regions are more sensitive to climate change and more easily impacted by future climate change and climate extremes than the northern regions, given this strong adaptation over the last 500 kyr or more. However, vegetation growth in these southern regions was significantly impacted by the recent, decadal region-wide drought (e.g. 2007–08), in which certain periods demonstrated no vegetation seasonality/phenology. It would be of interest to further explore the vulnerability or limits of resilience of these highly adapted savanna communities to future decadal or mega-droughts, as suggested recently by Ponce Campos et al. (2013).

The future climate of north Australia is predicted to be warmer and drier (Hennessy et al., 2004). Moreover, differences in future climate between the northern and southern ends of the transect study area are likely to occur. The dry season of the north may become wetter, with most warming expected to occur in the southern end of the NATT transect, where the climate is already very hot and dry (Hennessy et al., 2004). Over the 20th century, the frequency of extreme climate events, including extreme drought and heavy rainfall events, has already shown a statistically significant rising trend over several places in Northern Territory (Darwin, Waterloo, Brunette Downs and Tempe Downs), and this trend is expected to intensify in the future (Hennessy et al., 2004; Suppiah & Hennessy, 1996). Extended dry periods and associated increased VPD can reduce tree cover by almost 30% due to enhanced tree mortality in Australian savannas (Eamus, Boulain, et al. 2013; Eamus, Cleverly, et al., 2013; Fensham & Fairfax, 2007) and such an outcome will impact on regional carbon, water and energy balances.

Savannas are the most dynamic but relatively under-researched of global ecosystems. A more accurate representation of land surface phenology and vegetation dynamics across different savanna classes will improve the predictability of climate and land surface models and improve knowledge on the functioning of savanna ecosystems (Penuelas, Rutishauser, & Filella, 2009). In the IPCC 4th Assessment Report, Randall et al. (2007) noted that most climate models treat savannas as a single vegetation type and are thereby not capable of adequately capturing the variability of savanna structure, composition and function (Beringer, Hacker, et al., 2011; Beringer, Hutley, Hacker, Neininger, & Paw, 2011). These models are further unable to capture the seasonality of fluxes in savannas, which is a result of the complex interactions among rainfall, soil moisture, root distribution, and plant water uptake (Pitman, 2003). There is a key need to couple landscape flux measurements, remote sensing observations and ecological modeling towards a better understanding of savanna ecosytem functioning (Hill et al., 2011). Further investigations are needed to quantify these interactions and feedbacks between environmental factors and savanna phenology.

5. Conclusions

In this study, we investigated spatial variability and temporal variability in the phenology of savanna vegetation and relationships among phenology, rainfall and vegetation types across an ecological rainfall gradient (NATT). The validity of satellite retrieved phenological transition dates was assessed at three sites through comparisons with tower-based eddy flux measurements, confirming the utility of remote sensing to estimate the highly dynamic patterns of phenology in tropical mesic to semi-arid savannas.

Savanna phenological transition dates displayed different spatial patterns between the northern (mesic) and southern (xeric) parts of the study area. Along the northern transect study area, the start of the greening season (SGS), peak date (PGS) and end date (EGS) showed consistent but delayed trends from 12°S to 17.7°S. To the south of 17.7°S, this trend in the delay in phenology was absent and both spatial and inter-annual variances of phenology increased significantly.

We found that the variability of annual precipitation alone could explain 80% of the variance in phenology, and inter-annual variability in phenology was much higher in the larger southern semi-arid region. The semi-arid Mulga woodland/shrublands and hummock grassland showed the largest temporal variability, and were much more sensitive to variability in the amount of rainfall.

A good overall convergence was found between coarse resolution MODIS EVI and eddy flux tower measures of gross ecosystem production (GEP). Seasonal hysteresis in the relationship between MODIS EVI and flux tower GEP was particularly strong at the *Acacia* dominated woodlands sites. Such hysteresis effects, requiring different relationships during green-up and brown-down phases should be taken into account when up-scaling photosynthesis and transpiration from tower observations to regional scales using satellite observations.

We also found that increasing temporal variability in phenology coincided with decreasing tree/grass ratios. These findings suggest that the differential responses of savannas to climate variability may be a function of woody to herbaceous biomass, in which larger woody layer fractions promote higher stability and resilience to eventual future climate change. The pronounced spatio-temporal variations in savanna phenology encountered in this study strongly suggest that ecosystem models must include phenology to be reliable for the prediction of savanna ecosystem functioning.

Acknowledgments

This research was supported by ARC (DP1115479) grant entitled "Integrating remote sensing, landscape flux measurements, and phenology to understand the impacts of climate change on Australian landscapes" (Huete, CI), and the National Basic Research Program of China (No. 2012CB955304). The first author appreciates the financial support from the Chinese Scholarship Council, Ministry of Education, China. The works at Howard Springs and Alice Springs were supported by grants from the Australian Government's Terrestrial Ecosystems Research Network (TERN) (www.tern.gov.au). These works were also supported by OzFlux, AusCover, and the Australian Supersite Network, all parts of TERN and the latter of which is a research infrastructure facility established under the National Collaborative Research Infrastructure Strategy and Education Infrastructure Fund (Super Science Initiative) through the Department of Industry, Innovation, Science, Research and Tertiary Education. Funding from the National Centre for Groundwater Research and Training provided further support. We also sincerely thank the personnel involved with the maintenance and operation of the flux towers.

Appendix A. Supplementary data

Supplementary data associated with this article can be found in the online version, at http://dx.doi.org/10.1016/j.rse.2013.07.030. These data include Google maps of the most important areas described in this article.

References

Aban, J. L. E., & Tateishi, R. (2004). Application of Singular Spectrum Analysis (SSA) for the reconstruction of annual phenological profiles of NDVI time series data. *The 24th Proceedings of Asian Association of Remote Sensing. Section 11. Data Processing: data fusion* (http://www.a-a-r-s.org/acrs/proceeding/ACRS2004/Papers/DF204-7.htm (last accessed 18 May 2013)).

Ahl, D. E., Gower, S. T., Burrows, S. N., Shabanov, N. V., Myneni, R. B., & Knyazikhin, Y. (2006). Monitoring spring canopy phenology of a deciduous broadleaf forest using MODIS. *Remote Sensing of Environment*, *104*, 88–95.

Alexandrov, Theodore (2009). A method of trend extraction using singular spectrum analysis. *RevStat*, *7*, 1–22.

Anderson, A. N., Braithwaite, R. W., Cook, G. D., Corbett, L. K., Williams, R. J., Douglas, M. M., et al. (1998). Fire research for conservation management in tropical savannas: Introducing the Kapalga fire experiment. *Austral Ecology*, *23*, 95–110.

Archibald, S., & Scholes, R. J. (2007). Leaf green-up in a semi-arid African savanna-separating tree and grass responses to environmental cues. *Journal of Vegetation Science*, *18*, 583–594.

Asner, G. P., Wessman, C. A., & Archer, S. (1998). Scale dependence of absorption of photosynthetically active radiation in terrestrial ecosystems. *Ecological Applications*, *8*(4), 1003–1021.

Beard, J. S. (1981). Classification in relation to vegetation mapping. In A. N. Gillison, & D. J. Anderson (Eds.), *Vegetation classification in Australia* (pp. 97–106). Canberra CSIRO-Australian National Univ.: Press.

Beringer, J., Hacker, J., Hutley, L. B., Leuning, R., Arndt, S. K., Amiri, R., et al. (2011). SPECIAL—Savanna Patterns of Energy and Carbon Integrated across the Landscape. *Bulletin of the American Meteorological Society*, *92*, 1467.

Beringer, J., Hutley, L. B., Hacker, J. M., Neininger, B., & Paw, U. K. T. (2011). Patterns and processes of carbon, water and energy cycles across northern Australian landscapes: From point to region. *Agricultural and Forest Meteorology*, *151*, 1409–1416.

Borchert, R. (1994). Induction of rehydration and bud break by irrigation or rain in decidous trees of a tropical dry forest in Costa Rica. *Trees*, *8*(4), 198–204.

Bowman, D.M. J. S. (1996). Diversity patterns of woody species on a latitudinal transect from the monsoon tropics to desert in the Northern Territory, Australia. *Australian Journal of Botany*, *44*, 571–580.

Bowman, D.M. J. S., Brown, G. K., Braby, M. F., Brown, J. R., Cook, L. G., Crisp, M.D., et al. (2010). Biogeography of the Australian monsoon tropics. *Journal of Biogeography*, *37*(1), 201–216.

Bowman, D.M. J. S., Murphy, B., & Banfai, D. (2010). Has global environmental change caused monsoon rainforests to expand in the Australian monsoon tropics? *Landscape Ecology*, *25*(8), 1247–1260.

Bowman, D.M. J. S., Wilson, B.A., & Dunlop, C. R. (1988). Preliminary biogeographic analysis of the Northern Territory vascular flora. *Australian Journal of Botany*, *36*, 503–517.

Brown, M. E., de Beurs, K., & Vrieling, A. (2010). The response of African land surface phenology to large scale climate oscillations. *Remote Sensing of Environment*, *114*, 2286–2296.

Buermann, Wolfgang (2002). Analysis of a multiyear global vegetation leaf area index data set. *Journal of Geophysical Research*, *107*, 4646.

Chen, X., Hu, B., & Yu, R. (2005). Spatial and temporal variation of phenological growing season and climate change impacts in temperate eastern China. *Global Change Biology*, *11*, 1118–1130.

Chidumayo, E. N. (2001). Climate and phenology of savanna vegetation in southern Africa. *Journal of Vegetation Science*, *12*(6), 347–354.

Cook, G. D., Hatton, T. J., Pidsley, D., Herczeg, A. L., Held, A., O'Grady, A. P., et al. (1998). Water balance of a tropical woodland ecosystem, Northern Australia: A combination of micro-meteorological, soil physical and groundwater chemical approaches. *Journal of Hydrology*, *210*(1–4), 161–177.

Cook, G. D., & Heerdegen, R. G. (2001). Spatial variation in the duration of the rainy season in monsoonal Australia. *International Journal of Climatology*, *21*, 1723–1732.

Cook, G. D., Williams, R. J., Hutley, L. B., O'Grady, A. P., & Liedloff, A.C. (2002). Variation in vegetative water use in the savannas of the North Australian Tropical Transect. *Journal of Vegetation Science*, *13*(1), 413–418.

Donohue, R. J., McVicar, T. R., & Roderick, M. L. (2009). Climate-related trends in Australian vegetation cover as inferred from satellite observations, 1981–2006. *Global Change Biology*, *15*, 1025–1039.

de Beurs, K. M., & Henebry, G. M. (2005). Land surface phenology and temperature variation in the International Geosphere-Biosphere Program high-latitude transects. *Global Change Biology*, *11*(5), 779–790.

Duff, G. A., Myers, B. A., Williams, R. J., Eamus, D., O'Grady, A., & Fordyce, I. R. (1997). Seasonal patterns in soil moisture, vapour pressure deficit, tree canopy cover and pre-dawn water potential in a Northern Australian Savanna. *Australian Journal of Botany*, *45*(2), 211–224.

Eamus, D., Boulain, N., Cleverly, J., & Breshears, D.D. (2013). Global change-type drought-induced tree mortality: Vapour pressure deficit is more important than temperature per se in causing decline in tree health. *Ecology and Evolution*, http://dx.doi.org/10.1002/ece3.664.

Eamus, D., Cleverly, J., Boulain, N., Grant, N., Faux, R., & Villalobos-Vega, R. (2013). Carbon and water fluxes in an arid-zone Acacia savanna woodland: An analyses of seasonal patterns and responses to rainfall events. *Agricultural and Forest Meteorology*, *1–17*.

Eamus, D., Hutley, L. B., & O'Grady, A. P. (2001). Daily and seasonal patterns of carbon and water fluxes above a north Australian savanna. *Tree Physiology*, *21*, 977–988.

Eamus, D., & Prior, L. (2001). Ecophysiology of trees of seasonally dry tropics: comparisons among phenologies. *Advances in Ecological Research*, *32*, 113–197.

Easterling, D. R., Meehl, G. A., Parmesan, C., Changnon, S. A., Karl, T. R., & Mearns, L. O. (2000). Climate extremes: Observations, modeling, and impacts. *Science*, *289*, 2068–2074.

Egan, J. L., & Williams, R. J. (1996). Lifeform distributions of woodland plant species along a moisture availability gradient in Australia's monsoonal tropics. *Australian Systematic Botany*, *9*, 205–217.

Elsner, J. B., & Tsonis, A. A. (1996). *Singular spectrum analysis: A new tool in time series analysis.* New York Plenum Press.

Fensham, R. J., & Fairfax, R. J. (2007). Drought-related tree death of savanna eucalypts: Species susceptibility, soil conditions and root architecture. *Journal of Vegetation Science*, *18*, 71–80.

Ferreira, L. G., & Huete, A.R. (2013). Assessing the seasonal dynamics of the Brazilian Cerrado vegetation through the use of spectral vegetation indices. *International Journal of Remote Sensing*, *25*(10), 1837–1860.

Field, C. B., Lobell, D. B., Peters, H. A., & Chiariello, N. R. (2007). Feedbacks of terrestrial ecosystems to climate change. *Annual Review of Environment and Resources*, *32*, 1–29.

Fox, G. A. (1990). Drought and the evolution of flowering time in desert annuals. *American Journal of Botany*, *77*(11), 1508–1518.

Friedl, M. A., McIver, D. K., Hodges, J. C. F., Zhang, X. Y., Muchoney, D., Strahler, A. H., et al. (2002). Global land cover mapping from MODIS: Algorithms and early results. *Remote Sensing of Environment*, *83*(1–2), 287–302.

Frost, P., Medina, E., Menaut, J. C., Solbrig, O., Swift, M., & Walker, B. (1986). Responses of savannas to stress and disturbance: A proposal for collaborative programme of research. *Biology International*, *10*, 1–81.

Ghil, M., Allen, M. R., Dettinger, M.D., Ide, K., Kondrashov, D., Mann, M. E., et al. (2002). Advanced spectral methods for climatic time series. *Review of Geophysics*, *40*(1), 1003.

Gillison, A. N. (1981). *Towards a functional vegetation classification.* Vegetation classification in Australia, 30–41.

Glenn, E. P., Huete, A.R., Nagler, P. L., & Nelson, S. G. (2008). Relationship between remotely-sensed vegetation indices, canopy attributes and plant physiological processes: What vegetation indices can and cannot tell us about the landscape. *Sensors*, *8*, 2136–2160.

Griffin, G. F. (1984). Hummock grasslands. In G. N. Harrington, A.D. Wilson, & M.D. Young (Eds.), *Management of Australia's rangelands* (pp. 271–284). Melbourne CSIRO.

Guerschman, J. P., Hill, M. J., Renzullo, L. J., Barrett, D. J., Marks, A. S., & Botha, E. J. (2009). Estimating fractional cover of photosynthetic vegetation, non-photosynthetic vegetation and bare soil in the Australian tropical savanna region upscaling the EO-1 Hyperion and MODIS sensors. *Remote Sensing of Environment*, *113*(5), 928–945.

Hanan, N.P., Burba, G., Verma, S. B., Berry, J. A., Suyker, A., & Walter-Shea, E. A. (2002). Inversion of net ecosystem CO_2 flux measurements for estimation of canopy PAR absorption. *Global Change Biology*, *8*(6), 563–574.

Hanan, N.P., & Lehmann, C. E. R. (2011). Tree-grass interactions in savanna: Paradigms, contradictions and conceptual models. In M. J. Hill, & N.P. Hanan (Eds.), *Ecosystem function in Savannas. Measurement and modeling at landscape to global scales* (pp. 39–53). Boca Raton, Florida CRC Press.

Hennessy, K., Page, C., McInnes, K., Walsh, K., Pittock, B., Bathols, J., et al. (2004). *Climate change in the Northern Territory.* Melbourne University of Melbourne.

Higgins, S. I., Cartay, M.D.D., February, E. C., & Combrink, H. J. (2011). Is there a temporal niche separation in the leaf phenology of savanna trees and grasses? *Journal of Biogeography*, *38*(1), 2165–2175.

Hill, M. J., & Hanan, N. (2013). Current approaches to measurement, remote sensing, and modeling in savannas. *Ecosystem Function in Savannas* (pp. 515–545). CRC Press.

Hill, M. J., Román, M.O., Schaaf, C. B., Hutley, L., Brannstrom, C., Etter, A., et al. (2011). Characterizing vegetation cover in global savannas with an annual foliage clumping index derived from the MODIS BRDF product. *Remote Sensing of Environment*, *115*(8), 2008–2024.

Hmimina, G., Dufrene, E., Pontailler, J. Y., Delpierre, N., Aubinet, M., Caquet, B., et al. (2013). Evaluation of the potential of MODIS satellite data to predict vegetation phenology in different biomes: An investigation using ground-based NDVI measurements. *Remote Sensing of Environment*, *132*, 145–158.

House, J. I., & Hall, D. O. (2001). Productivity of tropical savannas and grasslands. *Terrestrial Global Productivity*, *33*, 363–400.

Huemmrich, K. F., Privette, J. L., Mukelabai, M., Myneni, R. B., & Knyazikhin, Y. (2005). Time-series validation of MODIS land biophysical products in a Kalahari woodland, Africa. *International Journal of Remote Sensing*, *26*(19), 4381–4398.

Huete, A.R. (1988). A soil-adjusted vegetation index (SAVI). *Remote Sensing of Environment*, *25*(3), 295–309.

Huete, A.R., Didan, K., Miura, T., Rodriguez, E. P., Gao, X., & Ferreira, L. G. (2002). Overview of the radiometric and biophysical performance of the MODIS vegetation indices. *Remote Sensing of Environment*, *83*, 195–213.

Huete, A.R., Didan, K., Shimabukuro, Y. E., Ratana, P., Saleska, S. R., Hutyra, L. R., et al. (2006). Amazon rainforests green-up with sunlight in dry season. *Geophysical Research Letters*, *33*(1), 06405.

Huete, A.R., Restrepo-Coupe, N., Ratana, P., Didan, K., Saleska, S. R., Ichii, K., et al. (2008). Multiple site tower flux and remote sensing comparisons of tropical forest dynamics in Monsoon Asia. *Agricultural and Forest Meteorology*, *148*(5), 748–760.

Hutley, L. B., & Beringer, J. (2011). Disturbance and climatic drivers of carbon dynamics of a north Australian tropical savanna. In M. J. Hill, & N.P. Hanan (Eds.), *Ecosystem function in savannas: Measurement and modeling at landscape to global scales* (pp. 57–75). Boca Raton, Florida CRC Press.

Hutley, L. B., Beringer, J., Isaac, P. R., Hacker, J. M., & Cernusak, L. A. (2011). A sub-continental scale living laboratory: Spatial patterns of savanna vegetation over a rainfall gradient in northern Australia. *Agricultural and Forest Meteorology*, *151*, 1417–1428.

Hutley, L. B., O'Grady, A. P., & Eamus, D. (2001). Monsoonal influences on evapotranspiration of savanna vegetation of northern Australia. *Oecologia*, *126*, 434–443.

Hüttich, C., Gessner, U., Herold, M., Strohbach, B. J., Schmidt, M., Keil, M., et al. (2009). On the suitability of MODIS time series metrics to map vegetation types in dry savanna ecosystems: A case study in the Kalahari of NE Namibia. *Remote Sensing*, *1*(4), 620–643.

Jenkins, J. P., Richardson, A.D., Braswell, B. H., Ollinger, S. V., Hollinger, D. Y., & Smith, M. L. (2007). Refining light-use efficiency calculations for a deciduous forest canopy using simultaneous tower-based carbon flux and radiometric measurements. *Agricultural and Forest Meteorology*, *143*(1–2), 64–79.

Jin, C., Xiao, X., Merbold, L., Arneth, A., Veenendaal, E., & Kutsch, W. L. (2013). Phenology and gross primary production of two dominant savanna woodland ecosystems in Southern Africa. *Remote Sensing of Environment*, *135*, 189–201.

Jones, D. A., Wang, W., & Fawcett, R. (2009). High-quality spatial climate data-sets for Australia. *Australian Meteorological and Oceanographic Journal*, *58*(12), 233–248.

Kanniah, K. D., Beringer, J., & Hutley, L. (2010). The comparative role of key environmental factors in determining savanna productivity and carbon fluxes: A review, with special reference to northern Australia. *Progress in Physical Geography*, *34*, 459–490.

Koch, G. W., Vitousek, P.M., Steffen, W. L., & Walker, B. H. (1995). Terrestrial transects for global change research. *Vegetatio*, *121*(12), 53–65.

Kondrashov, D., & Ghil, M. (2006). Spatio-temporal filling ofmissing points in geophysical data sets. *Nonlinear Processes in Geophysics*, *13*, 151–159.

Lo, F., Wheeler, M. C., Meinke, H., & Donald, A. (2007). Probabilistic forecasts of the onset of the North Australian wet season. *Monthly Weather Review*, *135*(10), 3506–3520.

Lu, H., Raupach, M. R., McVicar, T. R., & Barrett, D. J. (2003). Decomposition of vegetation cover into woody and herbaceous components using AVHRR NDVI time series. *Remote Sensing of Environment*, *86*(1), 1–18.

Martin, H. A. (2006). Cenozoic climatic change and the development of the arid vegetation in Australia. *Journal of Arid Environments*, *66*(8), 533–563.

McKeon, G. M., Day, K. A., Howden, S. M., Mott, J. J., Orr, D.M., Scattini, W. J., et al. (1990). Northern Australian savannas: Management for pastoral production. *Journal of Biogeography*, *355–372*.

Menzel, A., Sparks, T. H., Estrella, N., Koch, E., Rein Ahas, A. A., Alm-Kuebler, K., et al. (2006). European phenological response to climate change matches the warming pattern. *Global Change Biology*, *12*, 1969–1976.

Morton, S. R., Griffin, G. F., Short, J., Pearce, G., & Barker, R. D. (1995). Refugia for biological diversity in arid and semi-arid Australia: A report of the Biodiversity Unit of the Department of Environment, Sport and Territories. *Biodiversity series*Canberra ACT: Biodiversity Unit, Department of the Environment, Sport and Territories.

Nicholas, A.M. M., Franklin, D. C., & Bowman, D.M. J. S. (2011). Floristic uniformity across abrupt boundaries between Triodia hummock grassland and Acacia shrubland on an Australian desert sandplain. *Journal of Arid Environments*, *75*, 1090–1096.

NVIS (2007). *Australia's native vegetation — A summary of Australia's major vegetation groups 2007.*

O'Grady, A. P., Chen, X., Eamus, D., & Hutley, L. B. (2000). Composition, leaf area index and standing biomass of eucalypt open forests near Darwin in the Northern Territory, Australia. *Australian Journal of Botany*, *48*(5), 629–638.

O'Grady, A. P., Cook, P. G., Eamus, D., Duguid, A., Wischusen, J.D. H., Fass, T., et al. (2009). Convergence of tree water use within an arid-zone woodland. *Oecologia*, *160*(4), 643–655.

Penuelas, J., Rutishauser, T., & Filella, I. (2009). Phenology feedbacks on climate change. *Science*, *324*, 887–888.

Piao, S. L., Fang, J. Y., Zhou, L. M., Ciais, P., & Zhu, B. (2006). Variations in satellite-derived phenology in China's temperate vegetation. *Global Change Biology*, *12*, 672–685.

Pitman, A. J. (2003). The evolution of, and revolution in, land surface schemes designed for climate models. *International Journal of Climatology*, *23*(1), 479–510.

Ponce Campos, G. E., Moran, M. S., Huete, A.R., Zhang, Y., Bresloff, C., Huxman, T. E., et al. (2013). Ecosystem resilience despite large-scale altered hydroclimatic conditions. *Nature*, *1–5*.

Randall, D. A., Wood, R. A., Bony, S., & Colman, R. (2007). Climate models and their evaluation. In S. Solomon, D. Qin, M. Manning, Z. Chen, M. Marquis, K. B. Averyt, M. Tignor, & L. H. Miller (Eds.), *IPCC, 2007: Climate change 2007: The physical science basis. Contribution of working group I to the fourth assessment report of the intergovernmental panel on climate change* (pp. 589–662). Cambridge, UK Cambridge University Press.

Ratana, P., Huete, A.R., & Ferreira, L. (2005). Analysis of cerrado physiognomies and conversion in the MODIS seasonal-temporal domain. *Earth Interactions*, *9*, 1–22.

R Core Team (2013). *R: A language and environment for statistical computing.* Vienna, Austria R Foundation for Statistical Computing.

Richardson, A.D., & Hollinger, D. Y. (2005). Statistical modeling of ecosystem respiration using eddy covariance data: maximum likelihood parameter estimation, and Monte Carlo simulation of model and parameter uncertainty, applied to three simple models. *Agricultural and Forest Meteorology*, *131*, 191–208.

Roderick, M. L., Noble, I. A. N. R., & Cridland, S. W. (1999). Estimating woody and herbaceous vegetation cover from time series satellite observations. *Global Ecology and Biogeography*, *501–508*.

Running, S. W., & Hunt, E. R. (1993). Generalization of a forest ecosystem process model for other biomes, BIOME-BGC, and an application for global-scale models. In J. R. Ehleringer, & C. B. Field (Eds.), *Scaling physiological processes leaf to globe* (pp. 141–158). San Diego, USA Academic Press.

Scheiter, S., Higgins, S. I., Osborne, C. P., Bradshaw, C., Lunt, D., Ripley, B.S., et al. (2012). Fire and fire-adapted vegetation promoted C4 expansion in the late Miocene. *New Phytologist*, *195*(6), 653–666.

Scholes, R. J., & Archer, S. R. (1997). Tree-grass interactions in savannas. *Annual Review of Ecology and Systematics*, *28*, 517–544.

Scholes, R. J., & Parsons, D. A.B. (1997). *The Kalahari transect: research on global change and sustainable development in Southern Africa.* Global Change Report.

Scholes, R. J., & Walker, B. H. (1993). *An African savanna: Synthesis of the Nylsvley study.* Cambridge University Press.

Seager, R., Naik, N., & Vogel, L. (2013). Does global warming cause intensified interannual hydroclimate variability? *Journal of Climate*, *25*(9), 3355–3372.

Seghieri, J., Vescovo, A., Padel, K., Soubie, R., Arjounin, M., Boulain, N., et al. (2009). Relationships between climate, soil moisture and phenology of the woody cover in two sites located along the West African latitudinal gradient. *Journal of Hydrology*, *375*(8), 78–89.

Soudani, K., le Maire, G., Dufrene, E., Francois, C., Delpierre, N., Ulrich, E., et al. (2008). Evaluation of the onset of green-up in temperate deciduous broadleaf forests derived from Moderate Resolution Imaging Spectroradiometer (MODIS) data. *Remote Sensing of Environment*, *112*(5), 2643–2655.

Stockli, R., & Vidale, P. L. (2004). European plant phenology and climate as seen in a 20-year AVHRR land-surface parameter dataset. *International Journal of Remote Sensing*, *25*, 3303–3330.

Suppiah, R. (1992). The Australian summer monsoon: A review. *Progress in Physical Geography*, *16*(1), 283–318.

Suppiah, R., & Hennessy, K. J. (1996). Trends in the intensity and frequency of heavy rainfall in tropical Australia and links with the Southern Oscillation. *Australian Meteorology Magazine.*, *45*, 1–17.

Tucker, C. J., Townshend, J. R. G., & Goff, T. E. (1985). African land-cover classification using satellite data. *Science*, *227*(4685), 369–375.

Walker, J., & Gillison, A. N. (1982). Australian savannas. In B. J. Huntley, & B. H. Walker (Eds.), *Ecological studies* (pp. 5–24). Springer Berlin Heidelberg.

Walker, B. H., Steffen, W. L., Canadell, J., & Ingram, J. S. I. (1999). *IGBP Book Series No. 4. The Terrestrial Biosphere and Global Change: Implications for Natural and Managed Ecosystems. Synthesis Volume.* Cambridge, UK: Cambridge University Press.

Wang, D., & Liang, S. (2008). Singular spectrum analysis for filling gaps and reducing uncertainties of MODIS Land Products. Geoscience and remote sensing symposium, 2008. IGARSS 2008. *IEEE International*, *5*, 558–561.

Wang, D., Morton, D., Masek, J., Wu, A., Nagol, J., Xiong, X., et al. (2012). Impact of sensor degradation on the MODIS NDVI time series. *Remote Sensing of Environment*, *119*, 55–61.

White, M.A., de Beurs, K. M., Didan, K., Inouye, D. W., Richardson, A.D., Jensen, O. P., et al. (2009). Intercomparison, interpretation, and assessment of spring phenology in North America estimated from remote sensing for 1982–2006. *Global Change Biology*, *15*, 2335–2359.

White, M.A., & Thornton, P. E. (1997). A continental phenology model for monitoring vegetation responses to interannual climatic variability. *Global Biogeochemical Cycles*, *11*, 217–234.

Whitley, R., Macinnis-NG, C., Hutley, L., Berringer, J., Melanie, Z., Mathew, W., et al. (2011). Is productivity of mesic savannas light limited or water limited? Results of a simulation study. *Global Change Biology*, *17*(10), 3130–3149.

Williams, R. J., Duff, G. A., Bowman, D.M. J. S., & Cook, G. D. (1996). Variation in the composition and structure of tropical savannas as a function of rainfall and soil texture along a large-scale climatic gradient in the Northern Territory, Australia. *Journal of Biogeography*, *23*, 747–756.

Williams, R. J., Myers, B.A., Muller, W. J., Duff, G. A., & Eamus, D. (1997). Leaf phenology of woody species in a North Australian tropical savanna. *Ecology*, *78*(8), 2542–2558.

Woinarski, J., Mackey, B., Nix, H., & Traill, B. (2007). *The nature of northern Australia.* Canberra ACT Australian National University, E-Press.

Zhang, X. Y., Friedl, M.A., Schaaf, C. B., & Strahler, A. H. (2004). Climate controls on vegetation phenological patterns in northern mid-and high latitudes inferred from MODIS data. *Global Change Biology*, *10*, 1133–1145.

Zhang, X. Y., Friedl, M.A., Schaaf, C. B., Strahler, A. H., Hodges, J. C. F., Gao, F., et al. (2003). Monitoring vegetation phenology using MODIS. *Remote Sensing of Environment*, *84*, 471–475.

Zhang, X. Y., Friedl, M.A., Schaaf, C. B., Strahler, A. H., & Liu, Z. (2005). Monitoring the response of vegetation phenology to precipitation in Africa by coupling MODIS and TRMM instruments. *Journal of Geophysical Research*, *110*, 12103.